



## Combined oxygen-isotope and U-Pb zoning studies of titanite: New criteria for age preservation



Chloë E. Bonamici<sup>a,b,\*</sup>, C. Mark Fanning<sup>c</sup>, Reinhard Kozdon<sup>a</sup>, John H. Fournelle<sup>a</sup>, John W. Valley<sup>a</sup>

<sup>a</sup> Department of Geoscience, WiscSIMS, University of Wisconsin-Madison, 1215 W. Dayton St., Madison, WI 53706, USA

<sup>b</sup> Los Alamos National Laboratory, P.O. Box 1663, Los Alamos, NM 87545, USA

<sup>c</sup> Research School of Earth Sciences, The Australian National University, Jaeger III, Building 61, Mills Road, Canberra, ACT 0200, Australia

### ARTICLE INFO

#### Article history:

Received 9 September 2014

Received in revised form 2 February 2015

Accepted 2 February 2015

Available online 11 February 2015

Editor: K. Mezger

#### Keywords:

Titanite  
U-Pb dating  
Oxygen isotopes  
SIMS  
Zoning  
Diffusion  
Adirondack Mountains

### ABSTRACT

Titanite is an important U-Pb chronometer for dating geologic events, but its high-temperature applicability depends upon its retention of radiogenic lead (Pb). Experimental data predict similar rates of diffusion for lead (Pb) and oxygen (O) in titanite at granulite-facies metamorphic conditions ( $T = 650\text{--}800\text{ }^{\circ}\text{C}$ ). This study therefore investigates the utility of O-isotope zoning as an indicator for U-Pb zoning in natural titanite samples from the Carthage-Colton Mylonite Zone of the Adirondack Mountains, New York. Based on previous field, textural, and microanalytical work, there are four generations (types) of titanite in the study area, at least two of which preserve diffusion-related  $\delta^{18}\text{O}$  zoning. U-Th-Pb was analyzed by SIMS along traverses across three grains of type-2 titanite, which show well-developed diffusional  $\delta^{18}\text{O}$  zoning, and one representative grain from each of the other titanite generations. Type-2 and type-4 titanites show broadly core-to-rim decreasing  $^{206}\text{Pb}/^{238}\text{U}$  zoning, consistent with Pb diffusion at higher temperatures, and uniform or even slightly increasing  $^{206}\text{Pb}/^{238}\text{U}$  near grain rims, indicating subsequent recrystallization and/or new growth below the Pb blocking temperature. Type-2 and type-4 grain cores preserve ca. 1160 Ma ages that correlate with the anorthosite-mangerite-charnockite-granite magmatic phase of the Grenville orogeny, whereas grain rims give ca. 1050 Ma  $^{206}\text{Pb}/^{238}\text{U}$  ages that coincide with the culminating Ottawa phase. The type-3 titanite grain was sampled from a vein and yields  $^{206}\text{Pb}/^{238}\text{U}$  dates older than the syenite into which the vein was emplaced; accordingly, its  $^{206}\text{Pb}/^{238}\text{U}$  dates are interpreted as indicating excess uncorrected common Pb. Type-2 grains with recrystallized or shear-eroded margins show truncated or reversed  $^{206}\text{Pb}/^{238}\text{U}$  zoning but retain symmetrically decreasing  $\delta^{18}\text{O}$  zoning, consistent with grain margin modification following arrest of Pb diffusion but before arrest of O diffusion. It is concluded that O diffusion was slightly faster than Pb diffusion in Adirondack titanites at the conditions of (local) peak Ottawa metamorphism, making  $\delta^{18}\text{O}$  zoning a useful discriminator of closed-system age domains that did not suffer Pb loss. In addition, the small offset in the O and Pb partial retention zones constrains the timing and temperature of oblique-slip deformation along the Carthage-Colton Mylonite Zone: the details of porphyroblast microstructure and zoning data show that the oblique-slip shear zones were active at ca. 1050 Ma, with deformation initiating near the peak of Ottawa metamorphism at  $\sim 700\text{ }^{\circ}\text{C}$  and continuing through the O blocking temperature at  $\sim 550\text{ }^{\circ}\text{C}$ .

Published by Elsevier B.V.

### 1. Introduction

Titanite,  $\text{CaTi}[\text{SiO}_4](\text{O},\text{OH},\text{F})$ , is a common accessory mineral in alkaline igneous and many types of metamorphic rocks, and is a widely used U-Pb geochronometer (e.g., Tilton and Grunefelder, 1968; Mezger et al., 1991a; Verts et al., 1996; Frost et al., 2000; Kohn and Corrie, 2011; Spencer et al., 2013). The geologic problems to which titanite U-Pb geochronology can be applied depend on the amount and retention of radiogenic Pb within individual titanite grains. Titanite is more reactive than zircon, and it commonly recrystallizes. Thus, U-Pb

titanite dates are often interpreted as metamorphic ages, recording the time of pulsed magmatic heating, fluid infiltration, or deformation (e.g., Verts et al., 1996; Storey et al., 2007; Shang et al., 2010; Gao et al., 2011). Pb diffusion is also a well-documented phenomenon in titanite, and many titanite dates are interpreted to indicate the time of cooling of the host rock below a certain temperature (e.g., Mezger et al., 1991a; Flowers et al., 2006; Warren et al., 2012) – cited as being anywhere between  $\sim 500\text{--}800\text{ }^{\circ}\text{C}$  for typical geologic cooling rates (Mezger et al., 1991a; Cherniak, 1993; Scott and St-Onge, 1995; Verts et al., 1996; Kohn and Corrie, 2011; Spencer et al., 2013). In many cases, however, it remains unclear to what extent the U-Pb systematics of titanite are affected by diffusive Pb loss, and therefore the extent to which initial U-Pb titanite ages are disturbed (partially or wholly reset). Recognizing

\* Corresponding author at: Los Alamos National Laboratory, P.O. Box 1663, MS j514, Los Alamos, NM 87545, USA.

diffusive Pb loss and, specifically, intragrain U-Pb zoning arising from Pb loss is complicated by the multitude of processes that can produce zoning and the challenges of high-precision U-Pb microanalysis in titanite.

### 1.1. Zoning

In this work, U-Pb zoning refers to the spatial variations in the abundance and, thus, ratio of U and radiogenic Pb within a titanite grain. U-Pb zoning results in “age” zoning, or more accurately, measured-date zoning. Both the existence of U-Pb zoning and the processes that give rise to it complicate the geologic interpretation of measured dates. Generally, intragrain U-Pb zoning can arise from episodic crystal growth, recrystallization, or diffusion. Sequential addition of material to a mineral (growth) will produce domains with different U-Pb ages because the accumulation of radiogenic daughter began at different times within different growth domains. Growth ages therefore record times when P-T-X conditions were appropriate for titanite formation, either in magmas or during metamorphism. The breaking and reforming of bonds during recrystallization alters mineral U-Pb dates if some or all of the previously accumulated radiogenic Pb is lost from the recrystallized domain, with the result that different domains within a crystal can have different daughter/parent ratios. Recrystallized-titanite U-Pb dates thus typically indicate the timing of bond reorganization by reaction or deformation. Diffusion differentially redistributes Pb within a crystal, altering the daughter/parent ratio and, thus, U-Pb date; if the diffusive boundary conditions and physical diffusion pathways are known, this redistribution is a function of spatial position and is predictable (e.g., Carslaw and Jaeger, 1959; Dodson, 1973; Crank, 1975). Many dates determined from grains that have experienced Pb diffusion are not meaningful geologic ages, but the intragrain spatial distribution of these dates depends on a specific time-temperature path and therefore provides temporal constraints on the thermal history of the rock.

### 1.2. Analytical challenges

In the case of titanite, distinguishing among the potential zoning processes and their different geological implications requires both high-precision and high-spatial-resolution U-Pb analysis. Uranium and lead are incorporated as trace elements in titanite, where they substitute in the crystal structure for calcium (Higgins and Ribbe, 1976; Frost et al., 2000). Obtaining precise U-Pb dates in titanite presents the combined analytical challenges of low (trace) total U and Pb abundances and proportionally high non-radiogenic, or common, Pb abundance (Verts et al., 1996; Frost et al., 2000). In situ microanalytical techniques permit high-spatial-resolution U-Th-Pb isotopic measurements and sample very small material masses, on the order of a few nanograms. The precision of in situ U-Pb measurements in titanite is ultimately limited by sample size (i.e., counting statistics) and instrument sensitivity. Thus, it is generally easier to detect different age populations in titanite with in situ techniques than to precisely resolve subtle intragrain U-Pb zonation patterns.

Ideally, one would identify a geochemical surrogate for Pb in titanite – i.e., a species with similar diffusivity – that can be measured more precisely at the microscale. Experimental studies constrain the diffusivities of O, Pb, Zr, Nd, and Sr in titanite (Cherniak, 1993, 1995, 2006; Morishita et al., 1996; Zhang et al., 2006), and show that “wet” O and Pb diffusivities are similar over the temperature range ~650–800 °C (Fig. 1), which corresponds both to the estimated temperature range of partial retention of these elements and to upper-amphibolite to granulite-facies metamorphic conditions. Zhang et al. (2006) suggested the potential to link O-isotope composition with U-Pb date; however, this correlation has not previously been tested, either in experimental or natural samples.

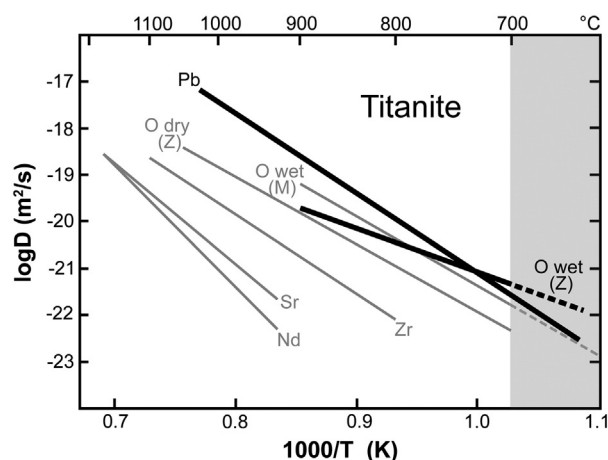


**Fig. 1.** Plot showing the experimentally determined Arrhenius relations for diffusion of various elements in titanite. Heavy lines are the Pb and wet O diffusion curves, which are inferred to be the relevant diffusivities for the current study. M = O diffusion data of Morishita et al. (1996); Z = oxygen diffusion data of Zhang et al. (2006). Modified from Zhang et al. (2006). Gray shading indicates the range of peak Ottawan metamorphic temperatures at Harrisville (Bohlen et al., 1985; Kitchen and Valley, 1995).

### 1.3. Beyond closure temperature

This study presents paired U-Th-Pb and O-isotope zoning profiles obtained by SIMS for six titanite grains from the Adirondack Mountains. The profiles reveal complex, intragrain elemental and isotopic variations that can nonetheless be deconvolved to identify the contributions of growth, recrystallization, and diffusion when they are considered in the context of field, microstructural, and additional geochemical data.

A major aim of the current study is to move towards meaningful interpretation of individual in situ (spatially resolved) U-Pb titanite dates in terms of petrologic processes and/or tectonic events. This is a departure from many studies of titanite, in which U-Pb dates are determined by bulk dissolution methods (e.g., Mezger et al., 1992; Flowers et al., 2006; Amelin, 2009) or populations of in situ analyses are pooled to obtain higher precision U-Pb dates (e.g., Aleinikoff et al., 2002, 2004; Kruckenberg et al., 2008; Warren et al., 2012). The implicit or explicit assumption of such studies is that the titanite grains, or the selected domains within a grain, are not zoned with respect to U-Pb systematics, or that the dispersion introduced into age determinations by zoning is small. This study demonstrates that titanite may exhibit significant U-Pb zoning, which manifests as a large spread of U-Pb dates in any given grain. More specifically, the current study demonstrates that Pb diffusion contributed substantially to the observed U-Pb zoning in the Adirondack titanites and must be considered when assigning geologic significance to their U-Pb dates.

The phenomenon of diffusive Pb loss in titanite, while potentially problematic for precise and accurate geochronology, is also an opportunity to extract information about a rock's time-temperature (T-t) history, beyond the traditional Dodson (1973) closure-temperature age. Zoning profiles contain information about the rate of cooling, the partial retention zone of the mineral, the final extent of disequilibrium, and compositional changes in the exchanging reservoirs (e.g., fluids). Thus, if the analytical limitations on the measurement of intragrain U-Pb zoning can be overcome, diffusion-related zoning patterns can be used to infer cooling paths and recognize geologically relevant ages amongst disturbed (inaccurate) ages.

This study investigates both the direct and indirect (surrogate) records of Pb diffusion in titanite, in the form of compositional zoning, as a means to improve the geologic interpretation of U-Pb titanite dates and to access more detailed information about the relative timing of structural and thermal events in the Adirondack Highlands. It is first established that Harrisville titanite U-Pb data, despite relatively large analytical errors, show petrologically significant variability, then it is considered how petrologic processes (growth, recrystallization, and

diffusion) can be inferred from that variability. Finally, information about the petrologic processes recorded in the grains is used, in conjunction with local and regional geologic data, to interpret the geologic significance of individual and grouped SIMS U–Pb titanite dates.

## 2. Geological setting and background

The Adirondack Mountains of northern New York expose polycyclic mid-crustal rocks of the 1.3–0.9 Ga Grenville orogeny (McLelland et al., 2010). Titanite grains for this study were sampled from two outcrops within the Carthage-Colton Mylonite Zone (CCMZ) near Harrisville, New York (Fig. 2; Cartwright et al., 1993; Lamb, 1993; Bonamici et al., 2011, 2014). The CCMZ is a major NNE-striking structure that juxtaposes the upper-amphibolite-facies Adirondack Lowlands to the northwest and the granulite-facies central Adirondack Highlands to the southeast (Fig. 2A). Titanites are hosted in the  $1164 \pm 11$  Ma (SHRIMP U–Pb zircon; Hamilton et al., 2004) Diana metasyenite, a member of the regionally extensive anorthosite–mangerite–charnockite–granite (AMCG) plutonic suite emplaced during the later part of the 1190–1140 Ma Shawinigan phase of the Grenville orogeny and subsequently deformed at granulite-facies metamorphic conditions during the 1090–1020 Ma Ottawa phase (McLelland et al., 2010). Previous studies found evidence for multiple deformation events within the broader CCMZ (Wiener, 1983; Baird and MacDonald, 2004), including an earlier oblique-slip event (Geraghty et al., 1981; Streepey et al., 2001; Johnson et al., 2004) and a later extensional event (Selleck et al., 2005). These events are also represented in the Harrisville outcrops (Bonamici et al., 2014), where an early protomylonite foliation ( $S_1$ ) is crosscut by  $\geq 100$  steeply dipping ultramylonite shear zones ( $S_2$ ), which are themselves transposed by a later, moderately dipping foliation ( $S_3$ ) (Fig. 3). The orientations of the  $S_2$  features are consistent with a conjugate network of shear zones accommodating oblique-slip motion. The moderately NW-dipping  $S_3$  is consistent with subsequent normal-sense motion. Although it is broadly agreed that the final stage of deformation along the CCMZ accommodated extension and exhumation of the Highlands from beneath the Lowlands (Mezger et al., 1991b; Selleck et al., 2005), the timing, kinematics, and significance of the earlier oblique-slip event are less well understood (Mezger et al., 1992; Streepey et al., 2000, 2001; Johnson et al., 2004).

A regional geochronologic study (Mezger et al., 1992) showed that, on average, U–Pb titanite ages are  $\sim 100$  m.y. older in the Lowlands (ca. 1150 Ma) than in the Highlands (ca. 1050 Ma). Generally, Lowlands ages are thought to record the time of Shawinigan metamorphism, whereas Highlands ages record peak Ottawa metamorphism (Mezger et al., 1992). The ranges of titanite U–Pb dates obtained, however, suggest

a complex mixture of crystallization and cooling ages within each region and within the intervening CCMZ. Mezger et al. (1992) recognized the possibility of Pb loss during Ottawa metamorphism but were unable to determine within the resolution of their bulk-dissolution analytical method whether titanite U–Pb heterogeneity reflected different periods of growth, recrystallization, and/or partial resetting by diffusion. Although peak Ottawa metamorphic temperatures in the central Highlands were as high as 800 °C (Bohlen et al., 1985; Storm and Spear, 2005), the Harrisville area likely remained at or below 700 °C during the Ottawa event (Kitchen and Valley, 1995), a temperature that falls within the commonly cited range of blocking temperatures for titanite (Mezger et al., 1991a; Scott and St-Onge, 1995; Verts et al., 1996).

Recently, SIMS analysis of  $\delta^{18}\text{O}$  in titanite from metasyenite outcrops in the CCMZ near Harrisville (Fig. 2B,C) revealed the presence of core-to-rim O-isotope zoning: twelve grains showed uniformly steep  $\delta^{18}\text{O}$  gradients within 50–200  $\mu\text{m}$  of the grain rims, consistent with arrested diffusive exchange of O (Bonamici et al., 2014). Numerical modeling of the O-isotope zoning profiles indicated relatively rapid cooling rates of 30–70 °C/my over the temperature range of 700–500 °C (Bonamici et al., 2014). Observed O-isotope zoning in the Harrisville titanite indicates that these grains are also candidates to preserve diffusion-related U–Pb zoning.

## 3. Methods

SIMS U–Th–Pb measurements were made on the SHRIMP II instrument at the Australian National University Research School of Earth Sciences (RSES) using a focused,  $\sim 4.5$  nA ( $\text{O}_2^-$ ) primary beam. Analysis spots were 29–40  $\mu\text{m}$  wide (longest dimension)  $\times$  2–3  $\mu\text{m}$  deep. Counts were acquired on both the sample and the BLR-1 titanite standard (Aleinikoff et al., 2007; Mazdab, 2009) in single-collector mode, with each analysis comprising seven scans through the masses on monovalent species  $^{200}\text{CaTi}_2\text{O}_4$ ,  $^{204}\text{Pb}$ ,  $^{206}\text{Pb}$ ,  $^{207}\text{Pb}$ ,  $^{208}\text{Pb}$ ,  $^{238}\text{U}$ ,  $^{248}\text{ThO}$ , and  $^{254}\text{UO}$ . U–Th–Pb data were collected during two separate analytical sessions; however, all measurements for a given grain were made during the same session. Six Harrisville titanites were analyzed *in situ* in five different 2.5-cm round mounts prepared from standard thin sections. To track instrumental drift and determine external U–Pb-age precision, one grain of U–Pb titanite standard BLR-1 was embedded toward the center of each thin-section sample mount. For each sample mount, BLR-1 was analyzed between 6 and 17 times during the traverse(s) of the selected sample grain(s). Data were reduced and isotope ratios calculated using SQUID software (Ludwig, 2012). Radiogenic  $^{206}\text{Pb}$  and  $^{207}\text{Pb}$  were calculated by correcting the measured  $^{204}\text{Pb}/^{206}\text{Pb}$  ratio in the samples with the measured Pb composition of the

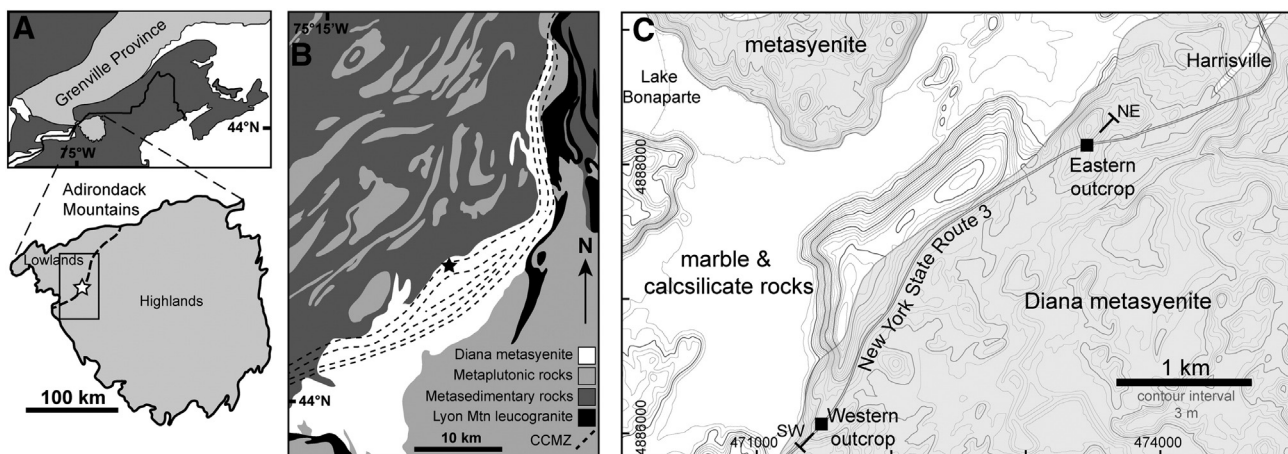
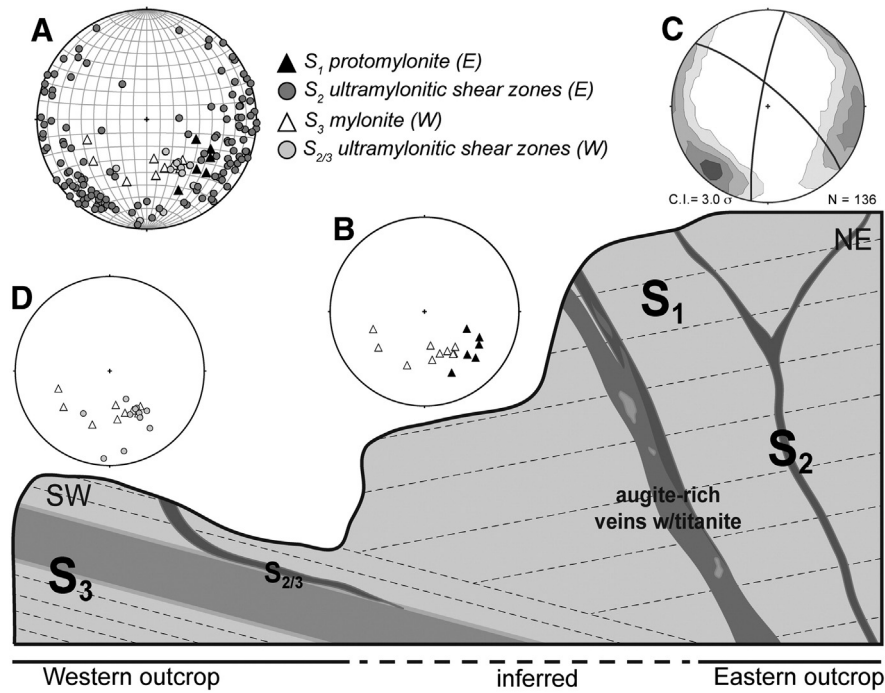


Fig. 2. Location of the Harrisville study area. (A) Position of the Adirondack Mountains, including the Highlands, the Lowlands, and the Carthage-Colton Mylonite Zone (CCMZ) within the larger Grenville Province. (B) Simplified geologic map of the vicinity around Harrisville, New York. (C) Locations of the two outcrops sampled in this study near the contact of the Diana metasyenite with the marbles of the northwestern Adirondack Lowlands. Ticks indicate the orientation of the structural cross-section in Fig. 3.



**Fig. 3.** Schematic NE-SW cross-section showing structures and crosscutting relations in the Harrisville outcrops. All structural data are displayed as poles to planes in lower-hemisphere equal-angle nets. (A) All measured structural data for the Eastern and Western outcrops. (B)  $S_1$  protomylonite and  $S_3$  mylonite “wallrock” foliations. (C) Contoured poles to planes of  $S_2$  ultramylonite shear zones, showing two dominant orientations that define a conjugate,  $\sim 60\text{--}120^\circ$  network. One representative plane for each of the two main orientations is also plotted. (D) Fabric measurements from the Western outcrop showing the similarity of the  $S_3$  mylonite and ultramylonite shear zones, consistent with transposition of  $S_2$  by  $S_3$ .

RSES long-term running calibration material, Broken Hills feldspar ( $^{206}\text{Pb}/^{204}\text{Pb} = 16.00$ ;  $^{207}\text{Pb}/^{204}\text{Pb} = 15.39$ ;  $^{208}\text{Pb}/^{204}\text{Pb} = 35.66$ ). Analysis pits were inspected by SEM, and a few dates were discarded (grayed out in figures) because of significant overlap with inclusions or another phase at a grain margin. All U-Th-Pb data are available in Appendix 1.

SIMS  $\delta^{18}\text{O}$  measurements were made on the CAMECA IMS-1280 ion microprobe at the University of Wisconsin-Madison WiscSIMS lab. Oxygen isotope measurements were collected along several traverses with a focused, 1.9–2.1 nA  $\text{Cs}^+$  primary beam. Analysis spots were 12–20  $\mu\text{m}$  long  $\times$  10–15  $\mu\text{m}$  wide  $\times$  1  $\mu\text{m}$  deep. Kita et al. (2009) and (Valley and Kita, 2009) give details of instrument tuning and operating conditions for O two-isotope analyses. Instrumental bias in the ion microprobe measurement of  $\delta^{18}\text{O}$  in titanite correlates linearly over the compositional range of interest ( $\sim 0.75\text{--}1.0$  formula atoms Ti) with the abundance of Ti in the octahedral site, which commonly also contains  $\text{Al}^{3+}$  and  $\text{Fe}^{3+}$ . Because the exact correction for bias varies with each analysis session, three well-characterized, chemically (major elements) and isotopically ( $\delta^{18}\text{O}$ ) homogeneous titanite standards (Bonamici et al., 2014) are measured and bracketed by analyses of the WiscSIMS in-house quartz standard (UWQ-1; Kelly et al., 2007) during each session. Following SIMS analysis, quantitative compositional data are collected within 10–30  $\mu\text{m}$  of every SIMS pit in the unknown by electron microprobe in order to calculate Ti formula atoms and apply the bias correction. All Harrisville SIMS  $\delta^{18}\text{O}$  data are reported Bonamici et al. (2014) and SIM  $\delta^{18}\text{O}$  data for the six titanite grains of this study are available in Appendix 2. Several analyses were discarded (grayed out in figures) because of significant overlap with inclusions or large fractures observed by post-analysis SEM imaging.

Quantitative (WDS) compositional data for traverses of type-1 and type-3 titanites and for the correction of SIMS  $\delta^{18}\text{O}$  bias were collected on the University of Wisconsin-Madison Cameca SX-51 electron microprobe. Point analyses were performed with a 15 keV accelerating voltage and a focused, 40-nA beam. In all but one sample, counts were collected for 14 major (Ca, Ti, Si), minor (Al, Fe, Na, Mg, Mn, F), and trace

(Zr, Hf, Y, Ce, Nd) elements with 10 s peak and 5 s background counting times. A Si peak shift was observed in titanite relative to the in-house jadeite standard and thus the Si peak position for all titanite analyses is based on Renfrew titanite (Bonamici et al., 2014). ZAF corrections and data reduction were performed with Probe for EPMA software (Donovan et al., 2012). Formula atom values were subsequently calculated from the ZAF-corrected element weight percent data by normalizing to three cations. All EPMA point data are reported in Appendix 3.

X-ray maps (Figs. 6, 8) were collected on three different electron microprobes in two different labs. The map of T2.1 was collected on the UW-Madison CAMECA SX-51 electron microprobe using a 25-kV accelerating voltage, 60-nA beam current, and a focused beam. Data were collected over the map area by stage motion with a 3  $\mu\text{m}$   $\times$  3  $\mu\text{m}$  pixel (step) size and 0.5 s dwell time per pixel. The strip maps of grains T2.2 and T4 (Fig. 6C,D) were collected on the CAMECA SX-50 at the University of Barcelona using a 20-kV accelerating voltage, 100 nA beam current, and a focused beam. Data were collected by stage motion with a scanning speed of 0.18 s per point. The smaller map area of T2.2 and the map of T2.3 were collected on the JEOL electron microprobe at the University of Barcelona using a 20-kV accelerating voltage, 100-nA beam current, and a focused beam. Data were gathered by stage motion with a 2  $\mu\text{m}$   $\times$  2  $\mu\text{m}$  pixel size and 250 ms dwell time per pixel. In all maps, (Figs. 6, 8) colors are scaled to raw X-ray counts and the range of quantitative element weight percent values was calculated from previous point analyses in representative low and high abundance locations. Image contrast was enhanced in all maps with Image J software to bring out subtle zoning features.

Electron backscatter diffraction maps (Figs. 7, 8) were collected with an Oxford/HKL EBSD detector on the UW-Madison Hitachi S-3400 scanning electron microscope. Maps were acquired on a 70° pre-tilted sample with a chamber pressure of 15–20 Pa, accelerating voltages of 15–20 keV, and a working distance of 23.5 mm. Data were collected over the map area by beam deflection, using a 3–4  $\mu\text{m}$  pixel (step) size. Only titanite was indexed. No post-processing image correction has been applied to the maps; white pixels are unindexed.

## 4. U-Th-Pb dates and zoning

### 4.1. Approach

Six titanite grains were selected from the outcrops near Harrisville, New York, in the Adirondack Mountains (Fig. 2) for SIMS U-Th-Pb traverses. Previously, four different generations (types) of titanite were distinguished and their relative timing determined on the basis of microstructural relations, major-minor element compositions and zoning, and  $\delta^{18}\text{O}$  zoning characteristics (Table 1; Bonamici et al., 2014). Type-1 (T1) and type-2 (T2) grains show diffusion-related  $\delta^{18}\text{O}$  zoning and are thus the optimal targets for comparison of O and Pb diffusion in the current study. Oxygen isotope zoning in type-3 (T3) and type-4 (T4) grains predominantly reflects recrystallization and late grain growth, which should also affect U-Pb ratios. The current study focuses on three type-2 titanite grains (T2.1, T2.2, T2.3) and one representative type-1, type-3, and type-4 grain each for U-Th-Pb SIMS analysis. SIMS U-Th-Pb data were collected along traverses parallel and either immediately adjacent to or in the same (repolished) location as previous SIMS  $\delta^{18}\text{O}$  traverses.

#### 4.1.1. Results: Concordia diagrams

Harrisville titanite grains have low or very low concentrations of U (5–75 ppm), low concentrations of radiogenic  $^{206}\text{Pb}$  (1–13 ppm), and moderate to high common Pb (2–20% of total Pb). The internal spot-to-spot precision (1SE) of  $^{206}\text{Pb}/^{238}\text{U}$  dates is  $\pm 17$ –51 m.y. (1.5–4.8%). The external accuracy of U-Pb dates as monitored by BLR-1 titanite standard is  $\pm 0.44$ –1.19% 2SD, depending on the sample mount (Appendix 1). Large uncertainties (standard errors) in  $^{207}\text{Pb}/^{206}\text{Pb}$  dates reflect extremely low  $^{207}\text{Pb}$  abundance. The more precise  $^{206}\text{Pb}/^{238}\text{U}$  dates are therefore used to investigate intragrain U-Pb zoning patterns. The results and discussion below deal primarily with the patterns of  $^{206}\text{Pb}/^{238}\text{U}$  dates within individual grains, which are compared using internal 1 $\sigma$  standard errors.

Regardless of grain type, Harrisville titanites give  $^{206}\text{Pb}/^{238}\text{U}$  date arrays that parallel the concordia (Fig. 4); within analytical error, these dates do not define clear linear discordia. The total range of  $^{206}\text{Pb}/^{238}\text{U}$  dates is 1212–978 Ma, with the majority of dates falling between 1180 and 1040 Ma. Every grain yields an array of  $^{206}\text{Pb}/^{238}\text{U}$  dates that spans a significant portion of, or nearly the entire, date range. Probability

density plots (Fig. 4) show multiple, poorly separated peaks or flat-topped plateaus.

Table 2 gives “ages” for the Harrisville titanite grains, calculated by pooling all the U-Pb dates for a given grain and applying conventional statistical methods. Only T1 yields statistically robust concordia and weighted-average ages. Of the remaining five grains, T2.3 and T3 give concordia ages with large MSWD values ( $>2$ ), while T2.1, T2.2 and T4 lack concordia age solutions. Weighted-average ages for all grains, except T1, also have large MSWDs. Dates from four of the six grains can be fitted with discordia age models, but although these model fits have low MSWD values, the calculated intercepts have very large uncertainties, and the lower intercept ages cannot be related to any known geologic events in the Adirondack region.

### 4.2. Results: $^{206}\text{Pb}/^{238}\text{U}$ date zoning profiles

All SIMS isotope zoning data, including U-Th-Pb and  $\delta^{18}\text{O}$  data, are shown in Fig. 5. T1, T2, and T4  $^{206}\text{Pb}/^{238}\text{U}$  date zoning profiles share a number of broadly similar features. In general, there is a progression from older dates in grain interiors to younger dates toward grain rims. Date profiles are commonly asymmetric, showing either different dates at opposing rims or, in the case of T4, showing rim zones with similar dates but different apparent widths. In all titanite types, including T3, date profiles show abrupt variations within grain interiors, such that a gradually varying trend is interrupted by a single significantly younger or older date. In detail, there are several zoning features that vary from type to type or from grain to grain.

Dates within the T1 grain are not distinguishable within measurement uncertainties. However, the  $^{206}\text{Pb}/^{238}\text{U}$  date profile across the largest domain of this divided grain (Fig. 5A) shows dates decreasing smoothly and symmetrically from ca. 1120 Ma in the domain center to ca. 1050 Ma at the domain edges. Large errors on T1  $^{206}\text{Pb}/^{238}\text{U}$  dates reflect extremely low U (4–6 ppm) and radiogenic  $^{206}\text{Pb}$  ( $\leq 1$  ppm) concentrations.

In T2 profiles (Fig. 5D), older dates (1140–1210 Ma) occur within grain interiors but do not always coincide with the grain center. In T2.1 (Fig. 5D-1), the oldest dates occur in lower left quadrant of the grain, and in T2.2 (Fig. 5D-2) the oldest dates occur on the left-hand side of the grain, extending all the way to the eastern grain margin. In the T2.3  $^{206}\text{Pb}/^{238}\text{U}$  date profile (Fig. 5D-3), a centralized domain of

**Table 1**  
Summary of U-Th-Pb and  $\delta^{18}\text{O}$  zoning data and interpretations for the Harrisville titanites.

Grains	Observations				Interpretations	
	Microstructure	Structural relations	$\delta^{18}\text{O}$ zoning	U-Pb zoning	$\delta^{18}\text{O}$ zoning process	U-Pb zoning process
T1	Porphyroclast within elongate aggregates of augite + quartz that define the S1 fabric; subgrain development	Pre-S1	Symmetric, core-to-rim decrease in each domain	None within error	Diffusion; minor dynamic recrystallization along left-hand margin	Diffusion
T2.1 T2.2 T2.3	Porphyroclasts in S2 ultramylonitic shear zones; deformation twins common but twin density varies within each grain; subgrain development locally near grain rims	Pre-S2	Symmetric, core-to-rim decrease; one asymmetric profile	Typically asymmetric, interior-to-rim decrease; increase at rim to form “tails” on T2.1 profile	Diffusion; profile truncation by later dynamic recrystallization in T2.3	Diffusion, including fast-path diffusion along subgrain and twin boundaries; later deformation-assisted dissolution-reprecipitation recrystallization of grain margins leading to structurally controlled profile truncation and profile “tails”
T3	Porphyroblast in augite-rich vein associated with S2 shear zones; few, widely spaced deformation twins	Syn-S2	Asymmetric; core-to-rim decrease	Nearly uniform interior with decreasing values across fractures; increasing rim “tail”	Diffusion	Diffusion along fractures (?) followed by minor rim growth; inheritance of excess (uncorrected) common Pb
T4	Rims overgrowing S3 fabric	Post-S3 rims	Nearly uniform core, increase at rims	Symmetric core-to-rim decrease with flat rim “tails”	Diffusion; significant modification of diffusion profile by subsequent dissolution-reprecipitation recrystallization; late rim growth	Diffusion; significant modification of diffusion profile by subsequent dissolution-reprecipitation recrystallization; growth of late rims

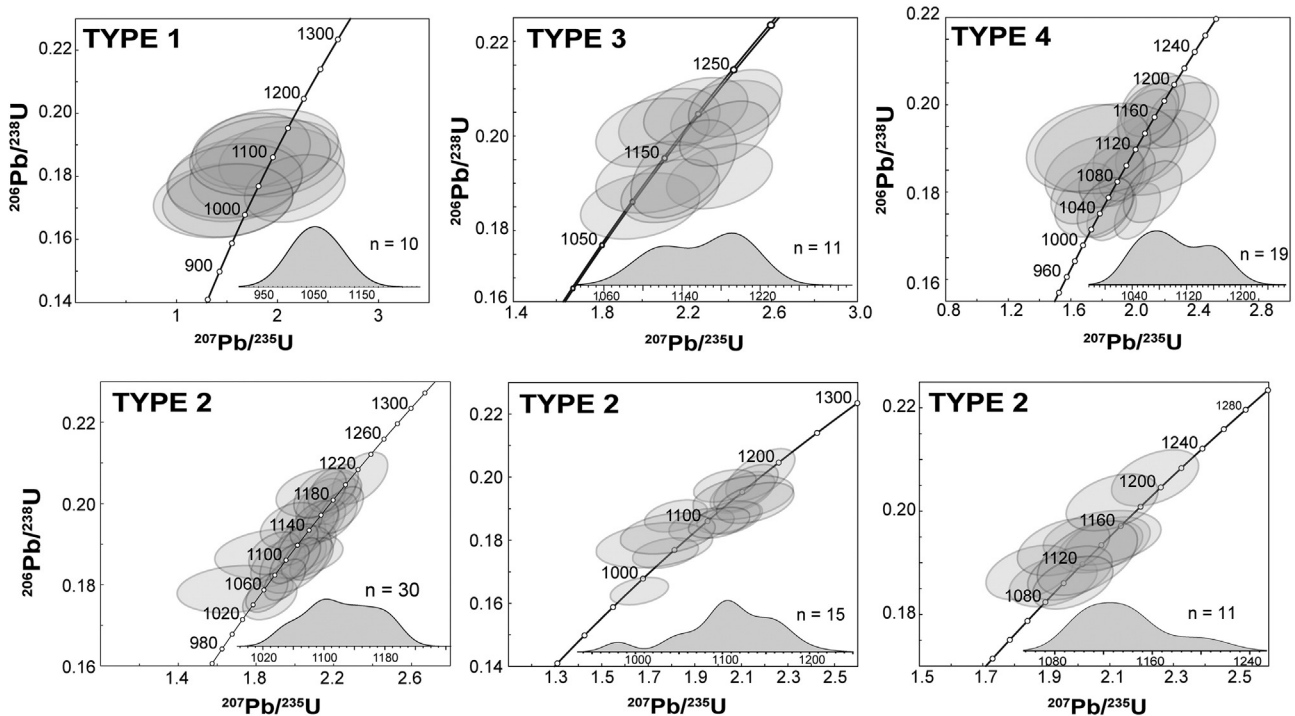


Fig. 4. Concordia diagrams for each of the six titanite grains in this study. Probability density distributions of  $^{206}\text{Pb}/^{238}\text{U}$  dates are shown in the lower righthand corner of each diagram.

old dates is bisected by a younger date. In T2 grains, the youngest dates along any given traverse occur at or near the current grain edges. The youngest T2 dates are ca. 1050 Ma (1045–1058 Ma), with the exception of one younger date (978 Ma) at the right edge of grain T2.2 (Fig. 5D-2).

The T3  $^{206}\text{Pb}/^{238}\text{U}$  date profile (Fig. 5B) differs from all other Harrisville titanite date profiles in that it is dominated by abrupt date variations with only very limited segments of the profile showing smooth, progressive date variations. Dates fall into two groups – an older group, comprising dates 1179–1212 Ma, and a younger group, comprising dates 1095–1138 Ma. Older dates occur in pristine-appearing regions between large, transgranular fractures, whereas analyses near these fractures commonly yield younger dates. Otherwise, there is no discernible spatial pattern to the dates – i.e., no core-to-rim younging pattern.

The oldest T4  $^{206}\text{Pb}/^{238}\text{U}$  dates (Fig. 5C) occur toward the grain center, where they define a plateau at 1160–1170 Ma. Dates decrease from the grain center toward the grain rims, where several analyses yield dates of ca. 1050 Ma. This flat profile segment is wider on one

side of the grain than the other. Within the well-defined central plateau, there are two younger dates that are uncorrelated with fractures, inclusions, or pits.

4.3. Discussion: SIMS U-Th-Pb dates

Despite the relatively large uncertainties on the Harrisville titanite SIMS U-Pb dates, several features of the data set indicate the presence of recognizable geological signals. First, U-Pb date profiles for five of the six titanite grains show spatially coherent patterns of variation that suggest zoning rather than analytical scatter. Second, large uncertainties and/or high MSWDs for conventional pooled-age calculations (Table 2) suggest that date scatter exceeds anticipated analytical errors (largely a function of counting statistics) and, thus, that titanite grains do not contain single concordant or discordant age populations. Finally, approximate “ages” for the Harrisville titanite grains (Table 2) are not consistent with relative ages inferred from grain textural relations (Table 1) – e.g., T1, the texturally oldest grain, gives the youngest

Table 2

“Ages”<sup>1</sup> calculated for six Harrisville titanite grains using all measured SIMS U-Pb dates for a given grain. See text for discussion.

Grain	n	Weighted Av. Age			Concordia Age			Model <sup>2</sup> Age				
		Date (Ma)	unc. <sup>3</sup> (Ma)	MSWD	Date (Ma)	unc. <sup>3</sup> (Ma)	MSWD	Upper Int. (Ma)	unc. <sup>3</sup> (Ma)	Lower Int. (Ma)	unc. <sup>3</sup> (Ma)	MSWD
T1	11	1069	26	0.57	1069	27	0.27					
T2.1	33	1128	15	4.7				1154	43	507	690	0.86
T2.2	15	1095	31	7.6				1121	210	936	750	0.84
T2.3	11	1137	23	3.3	1134	16	2.0					
T3	11	1162	28	2.6	1164	21	4.0	1250	190	116	3000	0.79
T4	19	1099	23	3.2				1141	87	152	1600	1.07

Calculated uncertainty reflects internal errors only and does not include the uncertainty in the BLR-1 standard U/Pb calibration listed in Appendix 1.

Note: Blank cells indicate age calculations that do not converge to a solution.

<sup>1</sup> Age calculations are performed to demonstrate the results of some conventional treatments of the data, but are not endorsed by the authors as being geologically accurate or relevant. Calculations assume that SIMS dates are n samplings of a single concordant or single discordant age population. All “ages” calculated using standard algorithms available in Isoplot 3.76 (Ludwig, 2012).

<sup>2</sup> All model ages are Isoplot Model 1 ages calculated using York’s algorithm; Monte Carlo age models give the same upper and lower intercepts but with asymmetric and significantly larger uncertainties.

<sup>3</sup> Because probability-of-fit is <0.05 for most ages, uncertainties are 95% confidence limits, except the uncertainty for the T1 concordia age, which is the 2σ internal error.

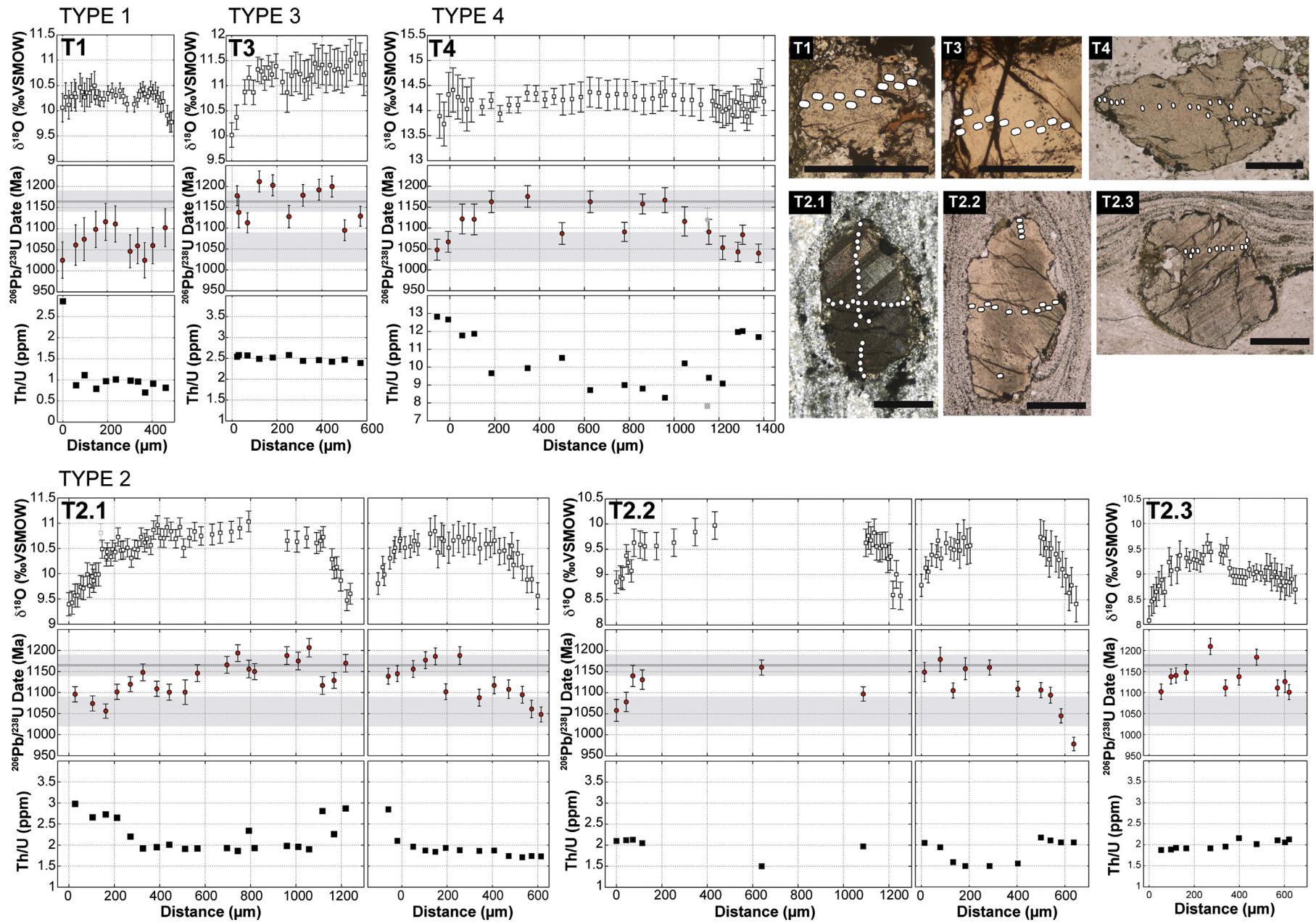


**Fig. 5.** SIMS  $\delta^{18}\text{O}$  and U-Th-Pb data plotted as a function of traverse distances for the six Harrisville titanite grains. Transmitted light images of each grain are shown in the upper right-hand corner; the scale bar for each image is 500  $\mu\text{m}$ . Locations of SIMS U-Pb analyses outlined by circles. SIMS  $\delta^{18}\text{O}$  traverses are not shown but parallel plotted U-Pb traverses. For each set of plots, the top plot is the  $\delta^{18}\text{O}$  zoning profile, the middle plot is the  $^{206}\text{Pb}/^{238}\text{U}$  date zoning profile, and the bottom plot is the Th/U zoning profile. Light gray bands on U-Pb plots indicate the age ranges for the Shawinigan (upper band) and Ottawan (lower band) phases of the Grenville orogeny. Dark gray line is the 1164 Ma U-Pb zircon age for the Diana metasyenite at Harrisville (Hamilton et al., 2004). (A) T1 grain. (B) T3 grain. (C) T4 grain. (D) T2 grains.

calculated ages, whereas the texturally younger T3 grain gives the oldest calculated ages. Thus, U-Pb date heterogeneity in the Harrisville titanite grains cannot be accounted for by analytical uncertainties alone, but must, in part, reflect zoning that developed during the formation and modification of titanite grains through petrologic processes.

The spread of  $^{206}\text{Pb}/^{238}\text{U}$  dates along the concordia and the poorly localized date peaks (Fig. 4) suggest that the Harrisville titanites preserve predominantly mixed or open-system dates. Mixed dates could result from analytical mixing of multiple, complexly intermingled age domains within each crystal, developed as a result of either irregular grain growth or heterogeneous grain recrystallization. Alternatively, open-system ages would reflect heterogeneous redistribution of radiogenic elements, specifically Pb, by diffusion.

To identify the records of specific petrologic processes in the U-Pb titanite data sets, more geochemical and structural data are required. Accordingly, the following three sections consider evidence of the contributions of different petrologic processes – growth, recrystallization, and diffusion – to the development of U-Pb zoning in titanite. Each section includes a brief introduction to the specific approach applied and a discussion of data presented in the section.

### 5. Growth zoning in titanite

#### 5.1. Approach

Growth-related Pb (and thus, date) zoning is determined by the spatial distribution of common Pb and (presumably immobile) radiogenic parent elements, U and Th. SIMS U-Th-Pb analysis yields measurements of U and Th concentration at each analysis site. Ideally, Th and U would be characterized at a higher spatial resolution, but mapping of these trace elements over the large area of the titanite grains is prohibitive. The problem of *in situ* trace element mapping is therefore addressed indirectly by comparing high-resolution major-minor element maps with Th/U (ppm) ratio profiles measured by SIMS (Fig. 6). The basis for this comparison is the coupled substitution required to charge balance Ca<sup>2+</sup> in a 7-fold-coordinated position between the <sup>V</sup>Ti and <sup>IV</sup>Si sites (Higgins and Ribbe, 1976; Frost et al., 2000). Incorporation of these ions requires coupled exchange of lower-charge ions on either the <sup>V</sup>Ti or O sites, or both, in order to maintain local charge balance (Higgins and Ribbe, 1976; Tiepolo et al., 2002; Mazdab, 2009). The most common exchange

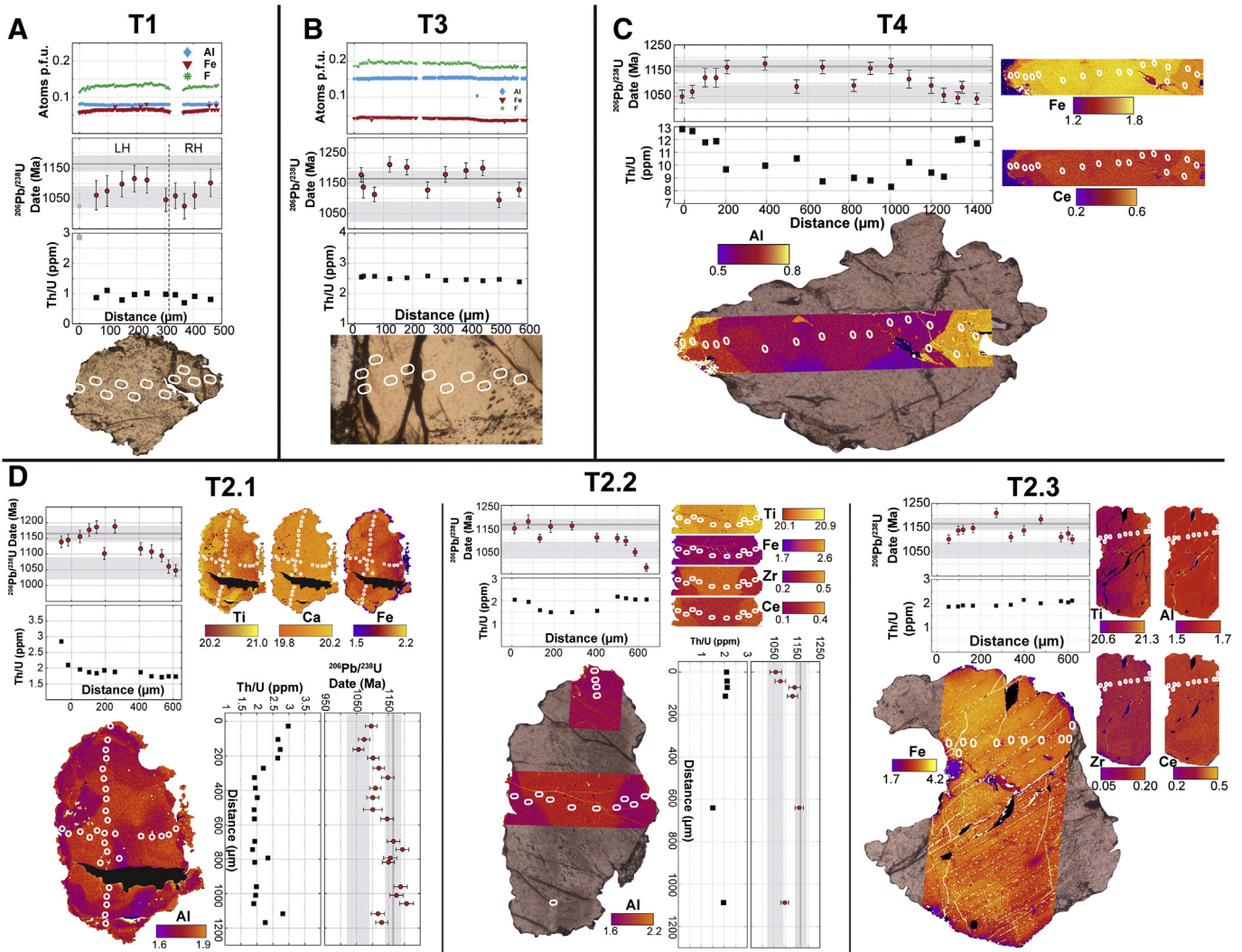


**Fig. 6.** Comparison of chemical composition and  $^{206}\text{Pb}/^{238}\text{U}$  age data for the six Harrisville titanite grains. Compositional line traverses only for T1 and T3; EPMA X-ray maps (full or partial) for all other grains. Color scale and corresponding values in element percent are given for each element map. Note that although color contrast has been enhanced to bring out subtle zoning features, actual chemical variations are small. Locations of SIMS U-Th-Pb analyses outlined by ellipses. For each grain, SIMS data plots are scaled to the grain; the middle or top plot is the SIMS  $^{206}\text{Pb}/^{238}\text{U}$  age zoning profile and the bottom plot is the Th/U zoning profile. As in the previous figure, the Shawanigan and Ottawan age ranges are indicated by the gray bands on the U-Pb age profiles. Gray data points were discarded because of pit irregularities, such as intersection of pits with large fractures or inclusions. (A) T1 grain, (B) T3 grain, (C) T4 grain, (D) T2 grains.

vectors involve minor elements  $\text{Al}^{3+}$  or  $\text{Fe}^{3+}$  on the  $^{\text{VI}}\text{Ti}$  site and coupled  $\text{OH}^-$  or  $\text{F}^-$  substitution on adjacent O sites (Oberti et al., 1991; Mazdab, 2009). We investigate the possibility that zoning arising from minor element substitutions on the  $^{\text{VI}}\text{Ti}$  site is correlated to, and may be used as a proxy for, zoning arising from trace element substitutions on the  $^{\text{VII}}\text{Ca}$  site. All quantitative EMPA data are available in Appendix 3.

## 5.2. Results: Chemical zoning

Chemical zoning in Harrisville titanites is subtle, with element abundances varying by a few tenths up to ~1 element weight percent (Fig. 6). Zoning may be either gradational or sharp but, in general, zoning of Ti, Al, Zr, and Ce is more sharply defined than zoning of Fe or F. T1, T3, and T2.3 are essentially unzoned with respect to major/minor elements. T4, T2.1, and T2.2 show patchy, gradational interior zoning with more sharply defined, though commonly irregular, rim zones. The largest-magnitude and most sharply defined elemental zoning occurs in T4.

Grain T1 has the lowest Th/U ratios (~1) and a nearly flat Th/U profile, with one outlying Th/U measurement at the left-hand grain rim (light gray symbols, Fig. 6A). T2 grains consistently show higher Th/U with ratios between 1.5 and 3 (Fig. 6D). T2.1 and T2.2 have Th/U zoning with lower Th/U ratios in the grain interiors and higher ratios at the grain margins. T3 yields very gradually decreasing Th/U with ratios between 2.6 at the grain rim to 2.4 within the grain interior (Fig. 6B). T4 shows a large range of Th/U ratios and very high Th/U ratios of 8–13 (Fig. 6C). Grain-interior Th/U ratios are more variable but are lower than grain-margin Th/U ratios.

Zoning on the  $^{\text{VI}}\text{Ti}$  site, Ce zoning on the  $^{\text{VII}}\text{Ca}$  site, and Th/U zoning are all strongly spatially correlated (Fig. 6; Appendix 3). These results suggest coupled-substitution trends and are consistent with crystal chemical studies indicating a linear correlation between the sizes of  $^{\text{VII}}\text{Ca}$  and  $^{\text{VI}}\text{Ti}$  sites in the titanite structure (Higgins and Ribbe, 1976; Oberti et al., 1991). We conclude that REE, Ti, Al, and Zr zoning are good proxies for U and Th growth zoning in the Harrisville titanites, and the zoning of these elements and U/Th ratio may be used to recognize growth-related date zoning.

## 5.3. Discussion: Growth zoning

In T1, T2, and T3 Harrisville titanites, there is no spatial correlation between growth zoning, as inferred from major and minor elements and Th/U ratio, and  $^{206}\text{Pb}/^{238}\text{U}$  date or  $\delta^{18}\text{O}$  zoning (Fig. 5). SIMS analyses that yield identical Th/U ratios may yield  $^{206}\text{Pb}/^{238}\text{U}$  dates that differ by as much as 140 million years (Fig. 6D, T2.1). Thus, growth zoning is not the dominant cause of the currently observed  $^{206}\text{Pb}/^{238}\text{U}$  date zoning in T1, T2, or T3 grains.

In contrast,  $^{206}\text{Pb}/^{238}\text{U}$  date and growth zoning are partially correlated in T4 (Fig. 6C). The correlation primarily reflects two distinct data populations – a population of older, highly variable, but lower Th/U analyses from the grain interior and a population of younger, less variable, higher Th/U analyses from the grain rims. Within the grain interior, Th/U and date variations are spatially decoupled. Within the left-hand grain rim, Th/U ratio covaries with dates; Thus,  $^{206}\text{Pb}/^{238}\text{U}$  date zoning in T4 reflects at least two distinct periods of grain growth to produce the grain interior and the grain rims.

## 6. Recrystallization

### 6.1. Approach

The term recrystallization broadly refers to the breaking and reforming of bonds with a concomitant change in crystal composition and shape. There are several possible recrystallization mechanisms. This work differentiates between the end-member mechanisms of deformation-induced (dynamic) recrystallization and dissolution-

precipitation recrystallization because they represent different geologic processes/events and produce zoning with different geochemical associations. Dynamic recrystallization commonly results in crystallographic reorientation, therefore its extent and relation to  $^{206}\text{Pb}/^{238}\text{U}$  date zoning in the Harrisville titanites can be assessed through transmitted light microscopy and high-resolution mapping of crystallographic orientation by electron backscatter diffraction (EBSD) (Fig. 7). The development of zoning by dissolution-precipitation recrystallization is atomistically similar to the development of growth zoning and occurs with little or no change in crystallographic orientation (assuming partial recrystallization). It is more difficult to recognize, but commonly produces gradational or patchy zoning, and abrupt variations in or truncations of otherwise smoothly varying zoning profiles.

### 6.2. Results: crystallographic orientation data

Both transmitted light microscopy and EBSD mapping show that each Harrisville titanite grain is dominated by a single crystallographic orientation. Nonetheless, in transmitted light, T1, T2, and T3 grains also show local development of undulose extinction, incipient mantle structure, and/or lamellar twinning. EBSD mapping confirms that undulose extinction reflects domains of gradational lattice misorientation, which increases from the grain interior toward the grain rim, reaching as much as 20° of relative misorientation in T1 (Fig. 7A) and ~5–10° of relative misorientation in T2 grains (Figs. 7D, 8C). Domains where misorientation exceeds 10° are functionally new grains, signaling incipient porphyroblast core-and-mantle development. All T2 grains are locally mantled by small titanite grains with well-defined grain boundaries and distinctly different crystallographic orientations (Fig. 7D). In transmitted light, twins appear as broad, commonly tapering lamellae with striated birefringence (Fig. 8A). EBSD mapping shows twins as very thin (1–5  $\mu\text{m}$  wide), tapering linear traces highly misoriented relative to the dominant crystallographic orientation (Fig. 8C,D). Twin density varies within grains and from grain to grain. Some grains have untwinned domains (Fig. 8), whereas others are pervasively twinned (Figs. 7, 8D–3). T3 and T2.3 show two intersecting sets of twins. T4 lacks optical indications of internal deformation and EBSD confirms that crystallographic orientation varies by less than 1° across the entire grain.

### 6.3. Discussion: Recrystallization

Microstructural and crystallographic orientation data demonstrate that the Harrisville titanites have not experienced penetrative dynamic recrystallization. In T1, T2, and T3 grains, crystallographic misorientation, subgrains, and twinning are, however, consistent with localized intracrystalline deformation to produce organized lattice defects. In the Harrisville titanite grains, the twinning is mechanical and develops as a precursor to larger-magnitude, more penetrative intracrystalline deformation. The youngest T1 date occurs where a SIMS analysis falls within a subgrain developed at the far left-hand grain margin (Fig. 7A). Within T2 porphyroclasts, subgrains and regions of high twin density also typically yield younger dates. In T2.1, the oldest  $^{206}\text{Pb}/^{238}\text{U}$  dates occur where the SIMS analytical traverses cross the largely untwinned SE quadrant of the grain, whereas the youngest dates and the largest date fluctuations occur where twins are abundant (Fig. 8D). Twins identified by EBSD in T2.1 also coincide with narrow, linear bands of alternating high and low Fe abundance visible in the Fe map (Fig. 8B). The spatial association of deformation twins with younger and more variable  $^{206}\text{Pb}/^{238}\text{U}$  dates, as well as with Fe anomalies, suggests that Pb and Fe abundances are affected by the presence of organized lattice defects like twin boundaries. In contrast, T4 shows no evidence of intracrystalline lattice deformation or dynamic recrystallization.

Two grains retain evidence for dissolution-reprecipitation zoning processes. T4 shows diffuse patchy zoning in the core and two abrupt

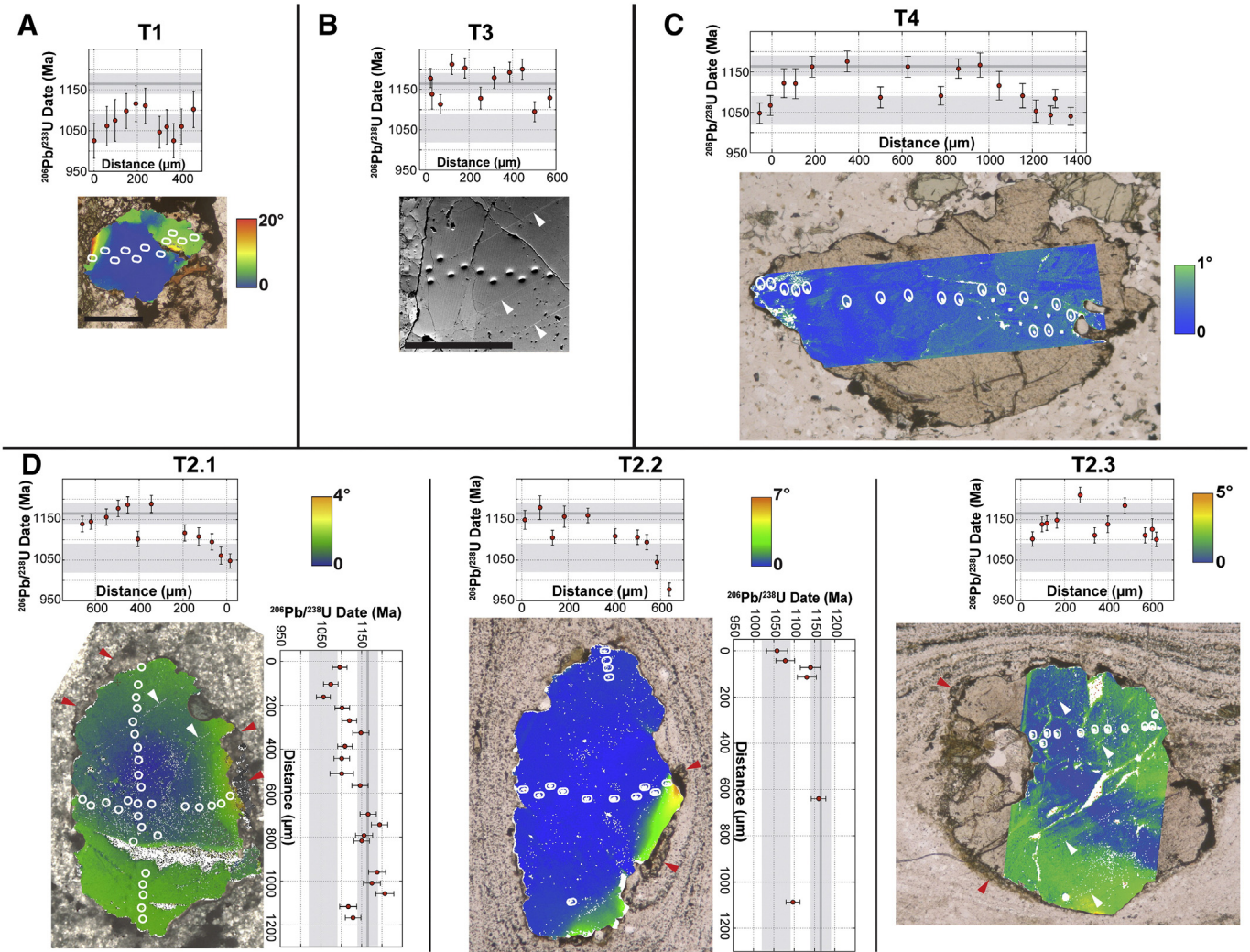


**Fig. 7.** Comparison of crystallographic orientation and  $^{206}\text{Pb}/^{238}\text{U}$  dates within the six Harrisville titanite grains. All images are EBSD relative misorientation maps superimposed on transmitted light photomicrographs, except B, which is an orientation contrast (forescatter) image. Color gradient in EBSD maps indicates degree of lattice misorientation relative to a point in the center of the grain. Grains are scaled with respect to each other and U-Pb date profile plots are scaled to each grain. Locations of SIMS U-Th-Pb analyses outlined by ellipses. White arrows point to thin deformation twins. Red arrows indicate fine-grained recrystallized rims. (A) T1 grain, (B) T3 grain, (C) T4 grain, (D) T2 grains.

age decreases in an otherwise well-defined central U-Pb date plateau (Fig. 6C). The northern and southern tips of T2.1 have several rim zones that are absent along the eastern and western grain margins (Fig. 6D-1) consistent with preferential material addition in the strain shadows of the grain and/or preferential removal of material at the foliation-parallel eastern and western margins during shearing. Although deformation clearly assisted the recrystallization, the rims in the strain shadows have the same orientation as the rest of the grain, indicating the dissolution-precipitation was the main recrystallization process.

## 7. Diffusion

### 7.1. Approach

If O and Pb diffusivities were similar at Ottawa peak metamorphic conditions, as predicted by hydrothermal experiments for wet conditions, then grains that record diffusive O isotope zoning should show symmetrically core-to-rim decreasing  $^{206}\text{Pb}/^{238}\text{U}$  date zoning profiles that mimic the shapes of  $\delta^{18}\text{O}$  profiles measured along the same traverse. This should also manifest as a positive correlation between  $\delta^{18}\text{O}$  and  $^{206}\text{Pb}/^{238}\text{U}$  age, such that higher (interior)  $\delta^{18}\text{O}$  values coincide with older U-Pb ages and lower (rim)  $\delta^{18}\text{O}$  values with younger

$^{206}\text{Pb}/^{238}\text{U}$  ages. Alternatively, differing O and Pb diffusivities will result in poorly correlated or uncorrelated  $\delta^{18}\text{O}$  values and  $^{206}\text{Pb}/^{238}\text{U}$  dates.

### 7.2. Results: SIMS $\delta^{18}\text{O}$ vs. SIMS U-Th-Pb

Within analytical uncertainties, T1  $^{206}\text{Pb}/^{238}\text{U}$  date profiles and  $\delta^{18}\text{O}$  profiles are uncorrelated. In general, T2 grains preserve  $^{206}\text{Pb}/^{238}\text{U}$  date profiles with similar overall shapes but greater internal complexity than their respective  $\delta^{18}\text{O}$  profiles (Fig. 5D). Four of the five T2 profiles show smooth, steeply decreasing  $^{206}\text{Pb}/^{238}\text{U}$  date profiles extending directly to at least one grain boundary. The T2.3  $^{206}\text{Pb}/^{238}\text{U}$  date profile terminates with a grain-boundary age of ca. 1100 Ma, whereas  $^{206}\text{Pb}/^{238}\text{U}$  profiles in grains T2.1 and T2.2 terminate with grain-boundary ages of ca. 1050 Ma. Three of the T2 profiles also have a pronounced asymmetry, such that the date at one boundary is different from the date at the opposing grain boundary (Fig. 5D). Nonetheless, T2 grains show positive  $\delta^{18}\text{O}$ -date correlations (Fig. 9D) that are strongest for analyses falling between 1050 and 1100 Ma. Above ~1150 Ma,  $\delta^{18}\text{O}$ -date correlations are ambiguous, reflecting grain interiors with nearly uniform  $\delta^{18}\text{O}$  but variable  $^{206}\text{Pb}/^{238}\text{U}$  dates. The T3  $\delta^{18}\text{O}$  and  $^{206}\text{Pb}/^{238}\text{U}$  age profiles differ (Fig. 5B) and are uncorrelated (Fig. 9B). Both the oldest and the youngest dates in T3 occur in the high- $\delta^{18}\text{O}$  grain interior. The T4  $\delta^{18}\text{O}$  and  $^{206}\text{Pb}/^{238}\text{U}$  date profiles both show an interior domain and a rim

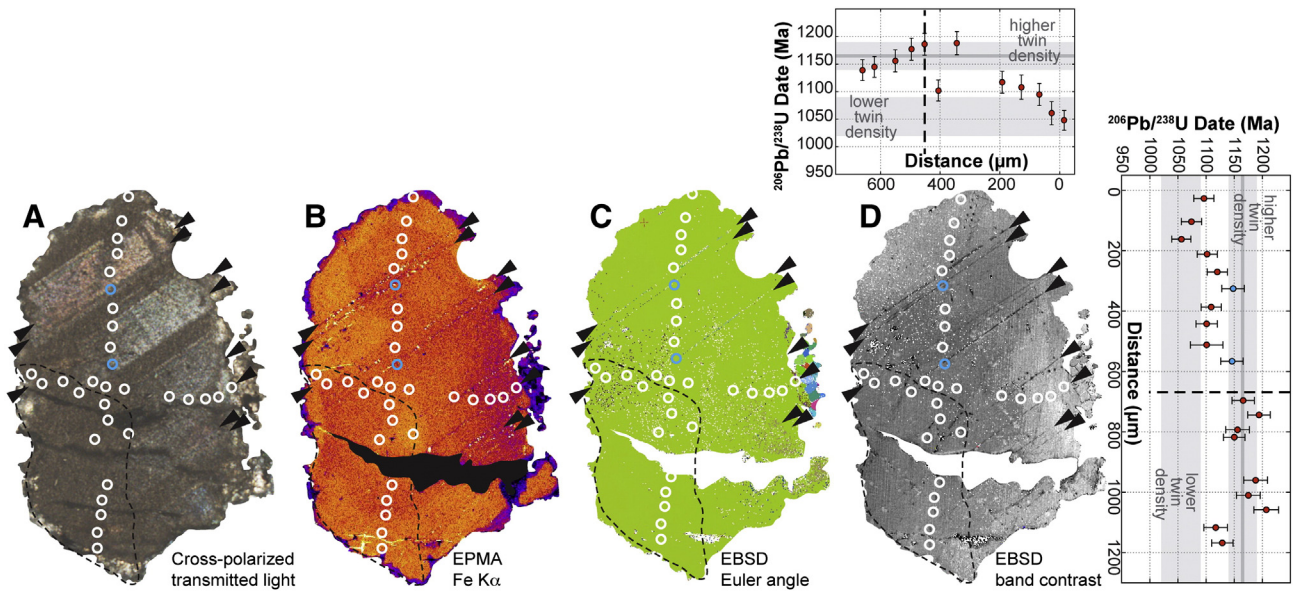


**Fig. 8.** Details of crystallographic orientation and Fe compositional variation in T2.1. In each image, small black arrows indicate a set of thin (1–5  $\mu\text{m}$  wide) deformation twin bands and the dashed line outlines a region of low twin density. Blue spots on images indicate analyses that fall directly on a twin band; corresponding data points on the plot are also blue. (A) Cross-polarized transmitted light photomicrograph showing broad lamellar deformation twins. (B) Fe K $\alpha$  X-ray map. Fe abundance increases from purple-red to orange-yellow. Thin deformation twins correlate to linear bands of alternating high- and low-Fe abundance. Similar features appear in the Fe K $\alpha$  X-ray map of T2.3 in Fig. 6D. (C) EBSD Euler angle map. Each color represents a distinct crystallographic orientation ( $\geq 10^\circ$  misoriented relative to nearest neighbor pixels). Thin twins show up as narrow zones of poorly indexed pixels. (D) EBSD band contrast map and U-Pb date profiles for comparison. Grayscale indicates the quality of the EBSD pattern, with darker colors indicating poorer quality. Twins show up as narrow zones of poor pattern quality. Note that the correlation of heterogeneous Fe distribution along the twins is consistent with twin boundaries acting as fast diffusion pathways.

domain as described above (Fig. 5C), but  $\delta^{18}\text{O}$  and dates are uncorrelated (Fig. 9C). The lack of correlation in T4 reflects relatively small  $\delta^{18}\text{O}$  variations across the grain but significant date differences between the core and rim growth domains and date variability within the core domain.

### 7.3. Discussion: diffusion

For T2 Harrisville titanites, the observed positive  $\delta^{18}\text{O}$ -date correlations confirm a first-order similarity in the shapes of  $\delta^{18}\text{O}$  and  $^{206}\text{Pb}/^{238}\text{U}$  date profiles and suggests that Pb diffusion was an important zoning process within these grains. The range and intragrain distribution of dates within T2 grains suggest partial diffusive resetting of

1170–1160 Ma crystallization ages by a ca. 1050 Ma reheating event. The relatively large T2 grains preserve 1180–1150 Ma core ages, which are indistinguishable within error from the  $1164 \pm 12$  Ma zircon crystallization age for the host syenite, and 1060–1045 Ma grain-boundary ages that are indistinguishable from the well-established age of peak Ottawa metamorphism. Both crystallographic domains within T1 are much smaller than the T2 grains and preserve younger  $^{206}\text{Pb}/^{238}\text{U}$  dates, consistent with more extensive Pb diffusion and age resetting.

Many of the second-order zoning features within T1 and T2 grains are also consistent with Pb diffusion. The two youngest  $^{206}\text{Pb}/^{238}\text{U}$  dates in the Harrisville grains – 978 Ma and 1020 Ma in T2.2 and T1,

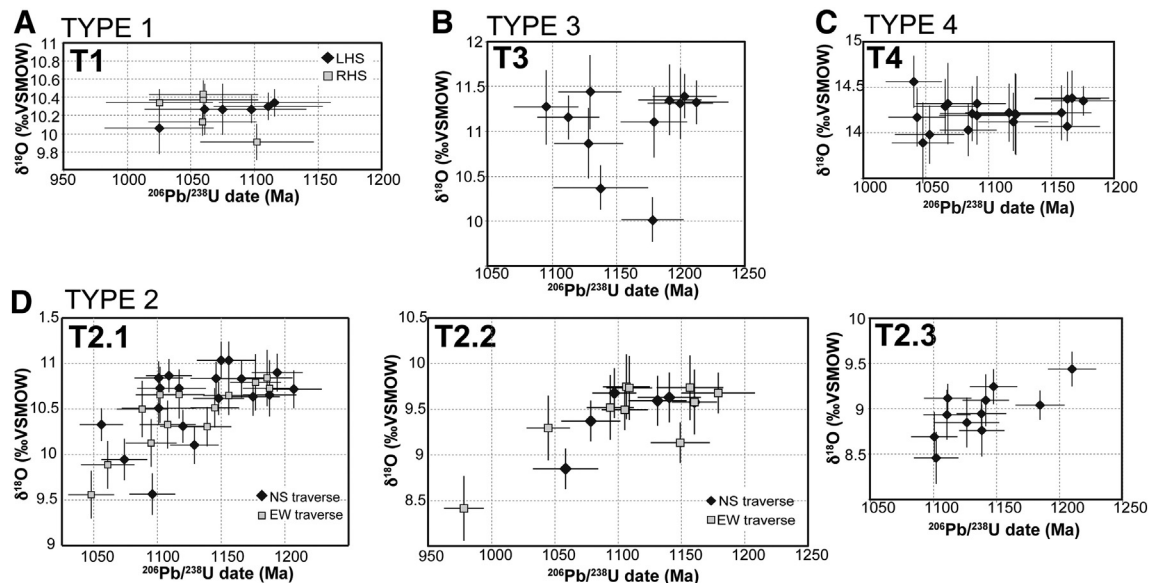


**Fig. 9.** Plots of  $\delta^{18}\text{O}$  vs.  $^{206}\text{Pb}/^{238}\text{U}$  date for each of the six Harrisville titanite grains. Correlated linear trends indicate  $\delta^{18}\text{O}$  and U-Pb date zoning profiles with similar shapes. (A) T1 grain, (B) T3 grain, (C) T4 grain, and (D) T2 grains.

respectively – occur at grain edges where the SIMS U–Pb analysis fell within dynamically recrystallized domains imaged by EBSD mapping (Fig. 7A, D–2). These young dates follow the decreasing date trend of the parent grain profiles and are thus consistent with more extensive Pb loss from a smaller diffusion domain during the same Pb loss event that affected the parent grain. Furthermore, twinned grains or twinned regions of grains preserve younger and/or more variable  $^{206}\text{Pb}/^{238}\text{U}$  dates. Twins appear to act as high-diffusivity pathways that effectively segment the grain into smaller diffusion domains in which Fe and Pb can undergo more extensive exchange. If twins also acted as high-diffusivity pathways for O, this interpretation accounts for the lower and more variable  $\delta^{18}\text{O}$  values in the densely twinned T2.3 grain (Figs. 5D, 6D, 7D).

The high- and low-Fe spots aligned along the twins suggest that these features do not, however, always act as high-diffusivity pathways but can become traps for diffusing Fe, and probably Pb, as temperatures and diffusivities drop. Evidence for radiogenic Pb trapping along twins appears in anomalously old dates where SIMS U–Th–Pb analysis pits directly intersect twin bands in T2.1 (Fig. 8, spots NS6 and NS10) and T2.3 (Fig. 6D). Oxygen isotope zoning profiles typically show more subtle fluctuations across twins than U–Pb ages, consistent with greater buffering of  $\delta^{18}\text{O}$  composition around the twins by the greater abundance of O relative to U and Pb.

The T3  $^{206}\text{Pb}/^{238}\text{U}$  date profile does not mimic the diffusion-dominated  $\delta^{18}\text{O}$  profile and the contribution of diffusion to the T3  $^{206}\text{Pb}/^{238}\text{U}$  zoning is unclear. The abrupt decreases in  $^{206}\text{Pb}/^{238}\text{U}$  date where the SIMS analyses cross transgranular fractures (Fig. 5B) could indicate that the fractures (or, more likely, a fracture-precursor planar deformation feature) were present during high-temperature metamorphism and acted as high-diffusivity pathways within the grain, or that the fractures were the loci of dissolution–reprecipitation recrystallization at lower temperature conditions. Th/U profiles give no indication of significant changes in chemical composition concurrent with abrupt  $^{206}\text{Pb}/^{238}\text{U}$  date variations, and thus dissolution–reprecipitation recrystallization seems less likely than Pb loss along fractures.

## 8. Synthesis and discussion

### 8.1. Summary of time–temperature history

Table 1 summarizes the observations of zoning and the interpretations of zoning processes in the four generations of Harrisville titanite. The T2 and T4 titanite grains retain evidence for  $^{206}\text{Pb}/^{238}\text{U}$  zoning as a result of diffusive Pb loss during the ca. 1050 Ma granulite-facies Ottawa event. In T2 and T4 grains, recrystallization, grain-margin erosion, and/or rim growth below the blocking temperature for Pb partially modified the  $^{206}\text{Pb}/^{238}\text{U}$  profiles. Nonetheless, the cores of these grains preserve ages that are consistent with early magmatic crystallization of titanite during the ca. 1160 Ma Shawinigan/AMCG event.

### 8.2. Uncorrected excess $^{206}\text{Pb}$

T3 preserves  $^{206}\text{Pb}/^{238}\text{U}$  dates that are incompatible with the geologic relations of the vein in which it crystallized. Many of the T3 dates (1192–1212 Ma) are older than both the earliest tectonic foliation ( $S_1$ ), which the vein crosscuts, and the Diana metasyenite itself, into which the vein was emplaced. The grain lacks textural or compositional evidence for an old xenocrystic core. Even if the Harrisville titanites contained unrecognized xenocrystic cores, their dates would most likely have been reset during incorporation into the Diana syenite magma, where temperatures would have been well above blocking for Pb diffusion in titanite. It is possible that the U/Pb ratio calibration of the BLR-1 standard grain in the SIMS mount with the T3 grain was spurious; however, this is unlikely. The  $2\sigma$  reproducibility (precision) of the BLR standard U/Pb ratio measured in the T3 mount is similar to or better than reproducibility in other mounts, suggesting that the dates obtained

in the T3 grain are not the result of a heterogeneous or anomalous BLR grain in the T3 sample mount (Appendix 1). We hypothesize instead that the common Pb composition of the vein titanite differed from the common Pb composition of the Broken Hills feldspar that was used correct the measured  $^{204}\text{Pb}/^{206}\text{Pb}$  ratio for common vs. radiogenic components. Specifically, the T3 grain may have incorporated Pb scavenged by vein fluids from the syenite wallrock, which would have been enriched in  $^{206}\text{Pb}$  and  $^{207}\text{Pb}$  relative to original magmatic common Pb composition (as approximated by the Broken Hills feldspar) by post-crystallization ingrowth. In other words, the old  $^{206}\text{Pb}/^{238}\text{U}$  dates in T3 reflect the presence of uncorrected, or excess, common  $^{206}\text{Pb}$ .

At least two lines of evidence support the idea that the titanite grain T3 contains uncorrected excess  $^{206}\text{Pb}$ . First, the similarity of pooled “ages” (Table 2) for grain T3 and the zircon U–Pb (magmatic) age of the syenite is consistent with the idea that the T3 Pb isotopic composition reflects the local Pb systematics of the syenite rather than the average Pb composition of the Grenville crust. Second, recrystallized and unrecrystallized vein titanites give different U–Pb dates. Previous TIMS and SIMS U–Pb studies of a dynamically recrystallized type-3 titanite grain – essentially an aggregate of sub-mm-sized grains – from the same Harrisville outcrop reported dates of 1079–1022 Ma (Heumann, 2004; Chappell et al., 2006), which are consistent with the geologic relations of these veins but still show a significant date spread, hinting at age mixing or variable Pb loss. The type-3 grain of this study was selected because it is largely undeformed (rare twins only) and was therefore deemed the best candidate in which to look for well-preserved diffusion-related Pb zoning. The differences in U–Pb dates between unrecrystallized and recrystallized vein titanites are consistent with expulsion of much or all excess uncorrected  $^{206}\text{Pb}$  during the recrystallization process.

There is currently no information published on the source of the Harrisville veins. However, the structural relations between veins and  $S_2$  shear zones indicate that the veins formed during the Ottawa event (Bonamici et al., 2014). Based on the inferred emplacement timing, mineralogy, and common alkalic alteration, the veins at the Harrisville site may be related to widespread, syn-extensional intrusion of the Lyon Mountain Granite and associated high-temperature hydrothermal alteration (Selleck et al., 2005; Valley et al., 2011). The proposed excess  $^{206}\text{Pb}$  in the T3 titanite grain of this study could have been incorporated into melts and then partitioned into late-stage aqueous fluids or scavenged by vein fluids from surrounding wall rocks.

Partial retention of excess common  $^{206}\text{Pb}$  may also account for the increasing  $^{206}\text{Pb}/^{238}\text{U}$  dates at the rim of T2.1. The microstructure of the grain indicates that these rims grew in the strain shadows of the titanite porphyroclast by dissolution of material from the foliation-parallel grain margins and reprecipitation along the foliation-perpendicular grain margins. If even some of the radiogenic Pb accumulated in the original crystal was incorporated into the reprecipitated rims, these rims would yield artificially old U–Pb dates.

### 8.3. Relative rates of O and Pb diffusion; age preservation

Both O and Pb diffusion must have occurred during the same high-temperature Ottawa metamorphic event, which is well documented for the Adirondack Highlands region in which the Harrisville study area is located. Yet  $^{206}\text{Pb}/^{238}\text{U}$  zoning profiles in T1, T2, and T4 grains do not exactly mimic  $\delta^{18}\text{O}$  profiles. Diffusion-related  $\delta^{18}\text{O}$  zoning extends to the current grain boundaries but diffusion-related U–Pb date zoning typically does not. Instead, grain rims show evidence of recrystallization- or growth-related age zoning (sometimes following grain-margin erosion) below the blocking temperature of Pb. This spatial, and presumably temporal, sequence of inferred zoning processes indicates that the blocking temperature of O was lower than the blocking temperature of Pb.

Overlap of O and Pb partial retention zones with O diffusion continuing to lower temperatures is consistent with experimental data showing

gradual divergence of the O and Pb Arrhenius curves for “wet” diffusion, with Pb becoming slower than O below  $\sim 725$  °C (Fig. 1; Zhang et al., 2006). Experimental data thus appear to successfully predict the relative diffusivities of O and Pb in natural hydrothermal samples that experienced cooling rates of  $\sim 30$ – $70$  °C/m.y. (Bonamici et al., 2011, 2014). The lower blocking temperature of O indicates that  $\delta^{18}\text{O}$  zoning can be a useful tool for identifying preserved U–Pb age domains within high-temperature titanites.

#### 8.4. Dating structures, fluids, and tectonic events at Harrisville

Despite Pb loss and partial age resetting in most Harrisville titanites, zoning data allow for the identification and direct dating of several events at the Harrisville location. The earliest-formed feature of T2 and T4 zoning profiles is the core-to-rim decreasing U–Pb dates and  $\delta^{18}\text{O}$  values, which reflects diffusive Pb loss. Plateau-like central regions of the profiles indicate that the grain interiors did not lose Pb; therefore, the grain-interiors of T2 and T4 titanites preserve their original crystallization ages. This conclusion is supported by the similarity of the grain-interior titanite ages (ca. 1160–1170 Ma) and U–Pb zircon age ( $1164 \pm 11$  Ma) from the same set of outcrops (Fig. 5C,D). Thus, despite pervasive granulite-facies metamorphism and significant Pb loss from grain rims, the pre-Ottawan magmatic crystallization age of the titanite is recovered by analysis of grain cores.

In the temperature and time interval between the blocking of O diffusion and the blocking of Pb diffusion, the T2 titanites experienced grain-shape modification, presumably as a result of deformation within the  $S_2$  shear zones. In T2.1 and T2.2 (Fig. 10A,B), some of the current grain edges represent the diffusive boundary condition and others that have been modified by post-diffusion recrystallization or growth can be located using chemical zoning and microstructural relations. Dates from the grain boundaries at the time of diffusion in T2 grains indicate that the network of oblique-slip  $S_2$  shear zones was active at ca. 1050 Ma. Shearing continued below the Pb blocking temperature, but  $\delta^{18}\text{O}$  zoning profiles that extend to the current grain boundaries indicate that  $S_2$  shearing had largely ceased by the time the system reached the O-blocking temperature. Only grain T2.3 shows evidence for truncation of its  $\delta^{18}\text{O}$  zoning profile (Fig. 5D-3) that would suggest some continued activity of  $S_2$  shear zones below the O-blocking temperature ( $\sim 550$  °C for the cooling rates and grain sizes of these titanites, see Bonamici et al., 2014). Thus,  $S_2$  shear zones were active at ca. 1050 Ma, coincident with peak Ottawan metamorphic conditions and continued to be active during cooling to  $\sim 500$  °C. The total duration of  $S_2$  shearing is constrained to 2–5 m.y. by previous modeling of  $\delta^{18}\text{O}$  diffusion zoning that found cooling rates of 30–70 °C/my (Bonamici et al., 2014). Oblique-slip shear zones have been documented within the CCMZ 20–30 km north of Harrisville, near Edwards and at Dana Hill, where they were dated at ca. 1040 Ma and interpreted as accommodating transpression

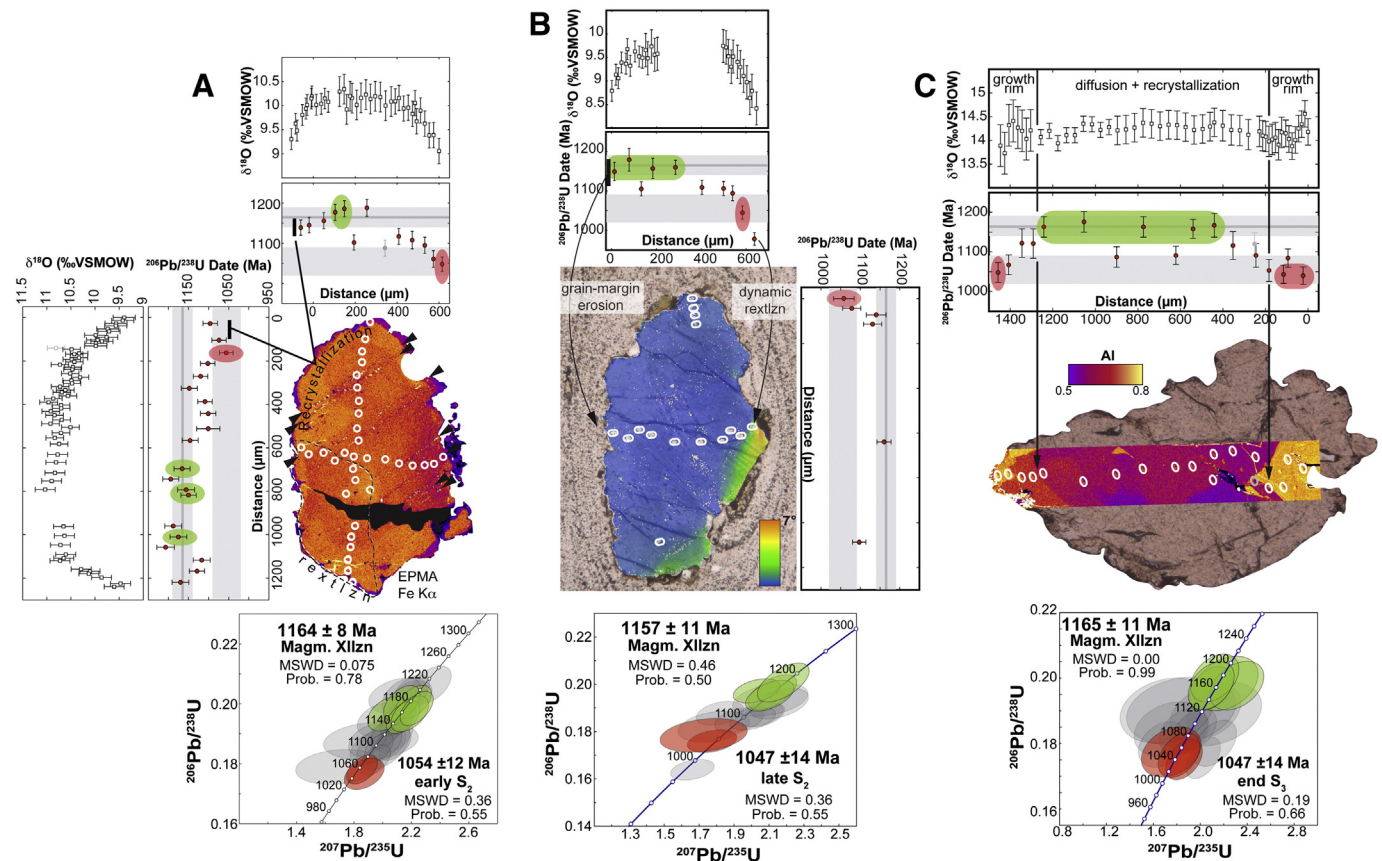


**Fig. 10.** Details of age interpretations from Harrisville titanite U–Pb date and  $\delta^{18}\text{O}$  zoning profiles. Combining the zoning and microstructural analyses allows for the identification of dates that are related to specific geologic events from the general date arrays for the each grain. For each grain, the oldest geologically relevant dates are highlighted in green on the U–Pb date profile and the associated concordia diagram. The youngest geologically relevant dates are highlighted in red on the U–Pb date profile and the associated concordia diagram. Note that all the listed dates and uncertainties are calculated with  $1\sigma$  internal errors. (A) T2.1 overlain by Fe Ka X-ray map. Recrystallization produced Fe zonation, as well as local truncation of the U–Pb date profiles and date profile “tails” reflecting partial to total Pb loss. The youngest dates are consistent with total Pb loss at an earlier grain boundary location during peak Ottawan metamorphism. Oxygen profiles reflect predominantly oxygen exchange by volume diffusion with the boundary condition at the current grain boundary. (B) T2.2 overlain by EBSD relative misorientation map. A diffusion-related U–Pb age profile was apparently truncated by shear-erosion of the grain margin below the blocking T of Pb but above the blocking T of oxygen, which shows a symmetric zoning profile. The oldest dates preserve the magmatic crystallization age of the titanite. The youngest grain-rim date signals substantial Pb loss from a small dynamically recrystallized domain at the grain edge. The grain-rim date immediately inboard of the rim is the actual date at the boundary of the larger grain and provides a minimum estimate for time of  $S_2$  shearing that formed that grain boundary. (C) T4 overlain by an Al K $\alpha$  map. Patchily zoned grain core preserves the original magmatic crystallization age of the grain. Late, sharply defined rims overgrow and thus provide a minimum date for the  $S_2$  fabric, as well high- $\delta^{18}\text{O}$  fluid infiltration evidenced by increasing  $\delta^{18}\text{O}$  in the rim overgrowths.

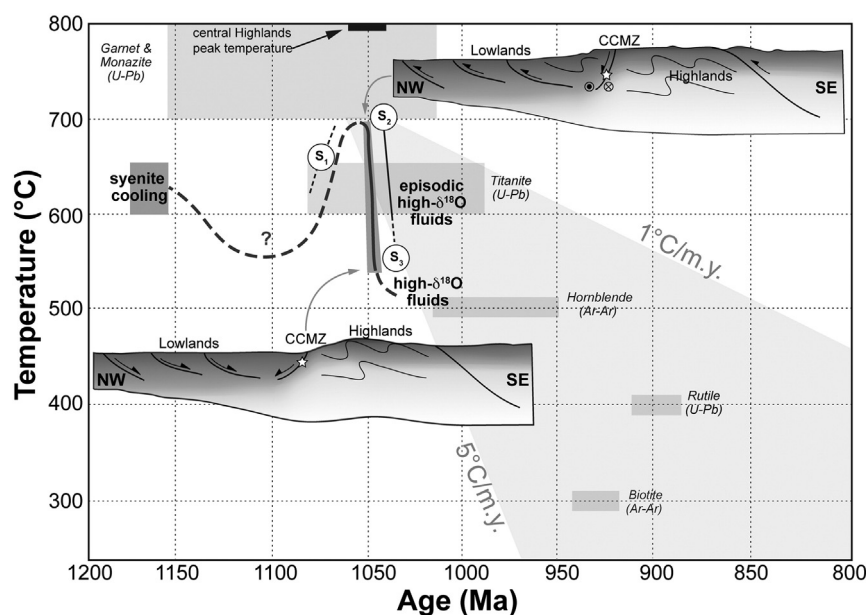


**Fig. 11.** Time-temperature plot summarizing structural and metamorphic events at Harrisville in relation to late-Grenville gravitational collapse. Medium gray boxes are thermochronology constraints for the Highlands cooling history (Mezger et al., 1991a, 1992; Streepey et al., 2000, 2001; Dahl et al., 2004). Light gray triangular envelope defined by the 1 °C/m.y. and 5 °C/m.y. cooling curves outlines the long-term average cooling rates and history of the Highlands. Dark gray boxes and paths indicate segments of the cooling history determined from titanite zoning data of this study and Bonamici et al. (2014). Path is dashed where uncertain and solid where inferred from titanite data. Relative timing of the three fabrics and fluid infiltration are shown by label. Schematic cross-sections through the Ottawa orogen show the inferred configuration at peak Ottawa metamorphic conditions (upper section) and the inferred configuration at the end of rapid cooling and collapse (lower section).

within the Ottawa orogen (Streepey et al., 2001; Johnson et al., 2004; Johnson and Selleck, 2005). The kinematics of the  $S_2$  shear zones are poorly constrained as they lack a well-developed lineation. The slightly older dates obtained on  $S_2$  shear zones at Harrisville may indicate diachroneity of oblique-slip motion along different parts of the CCMZ.

Rims of the T4 grain that overgrow the  $S_3$  fabric yield  $1047 \pm 14$  Ma (Fig. 10C), a minimum age for  $S_3$  fabric development and indistinguishable within error from the age of the  $S_2$  shear-zone network. It appears that the  $S_2$  and  $S_3$  fabrics formed in rapid succession over a period  $\leq 10$  my, and possibly  $\leq 5$  my. Oxygen isotope zoning in T2 grains shows that at least the  $S_2$  shear zones formed concurrently with rapid cooling brought on by tectonic exhumation of the Adirondack Highlands from beneath the Lowlands along the CCMZ (Bonamici et al., 2011, 2014). Thus, the  $S_2$  and  $S_3$  fabrics are the structural record at Harrisville of late-Ottawan gravitational collapse (Fig. 11), which was waning or had ceased by ca. 1050 Ma. Finally, the late T4 rims also show higher  $\delta^{18}\text{O}$  values (Fig. 5C) consistent with growth either in the presence of a high- $\delta^{18}\text{O}$  fluid or in rocks that had previously exchanged with a high- $\delta^{18}\text{O}$  fluid. Therefore, the ca. 1050 Ma rim age also places a lower age constraint on the timing of high- $\delta^{18}\text{O}$  fluid infiltration at Harrisville. If nearby high- $\delta^{18}\text{O}$  marbles of the Adirondack Lowlands were the source of the high- $\delta^{18}\text{O}$  fluids, then the T4 rim age suggests that the Highlands and Lowlands were juxtaposed across the CCMZ prior to  $\sim 1050$  Ma, somewhat earlier than proposed by Mezger et al. (1992) and Streepey et al. (2001) but consistent with the timing of juxtaposition and extension proposed more recently by Selleck et al. (2005).

## 9. Conclusions

- U-Pb date zoning in titanite reflects a combination of diffusion, recrystallization, and growth. These processes can be distinguished by comparing compositional and textural data sets collected at similar spatial resolution.
- Diffusion of O was slightly faster than the diffusion of Pb at the local peak and high-temperature cooling conditions of Ottawa metamorphism, consistent with experimental data at 650–800 °C. Thus,

$\delta^{18}\text{O}$  zoning is a useful tool to identify regions of preserved and reset U-Pb dates in titanite, and therefore to evaluate titanite ages.

- Several of the Harrisville titanites retain ca. 1160 Ma dates consistent with a preserved magmatic crystallization age, despite a pervasive granulite-facies metamorphic overprint at ca. 1050 Ma. These are the first distinctly AMCG titanite ages reported from the Adirondack Highlands.
- The offset in the partial retention zones of O and Pb in titanite can be utilized in conjunction with microstructural information to date specific geologic events at Harrisville. Oblique-slip  $S_2$  shear zones formed initially at the peak of Ottawa metamorphism and continued to actively shear for 2–5 m.y. during the period of rapid cooling that followed (Bonamici et al., 2014). The extension-related  $S_3$  deformation fabric developed very shortly after or at the tail end of  $S_2$  deformation and ceased by ca. 1050 Ma, when high- $\delta^{18}\text{O}$  fluids infiltrated along the Carthage Colton Mylonite Zone.

Supplementary data to this article can be found online at <http://dx.doi.org/10.1016/j.chemgeo.2015.02.002>.

## Acknowledgements

We thank Noriko Kita, Kouki Kitajima, Ariel Strickland, and Jim Kern for assistance in the WiscSIMS lab and Brian Hess for sample preparation. We thank Dr. Xavier Llovet for instrument time at the University of Barcelona. Laurel Goodwin and Brad Singer provided helpful comments on this manuscript. John Craven and John Aleinikoff provided titanite standards. John Aleinikoff, Andrew Kylander-Clark, and an anonymous individual provided thorough, helpful reviews. This material is based upon work supported by the U.S. National Science Foundation (award EAR-0838058), the U.S. Department of Energy, Office of Basic Energy Sciences under Award Number DE-FG02-93ER14389, and Geological Society of America student research grant 9224–10. WiscSIMS is partially supported by NSF-EAR-1053466 and – 1355590.

## References

- Aleinikoff, J.N., Wintsch, R., Fanning, C.M., Dorais, M., 2002. U–Pb geochronology of zircon and polygenetic titanite from the Glastonbury Complex, Connecticut, USA: an integrated SEM, EMPA, TIMS, and SHRIMP study. *Chem. Geol.* 188, 125–147.
- Aleinikoff, J.N., Horton, J., Drake, A., Wintsch, R., Fanning, C.M., Yi, K., 2004. Deciphering multiple Mesoproterozoic and Paleozoic events recorded in zircon and titanite from the Baltimore Gneiss, Maryland: SEM imaging, SHRIMP U–Pb geochronology, and EMP analysis. *Geol. Soc. Am. Mem.* 197, 411–434.
- Aleinikoff, J.N., Wintsch, R., Tollo, R.P., Unruh, D.M., Fanning, C.M., Schmitz, M.D., 2007. Ages and origins of rocks of the Killingworth dome, south-central Connecticut: Implications for the tectonic evolution of southern New England. *Am. J. Sci.* 307, 63–118.
- Amelin, Y., 2009. Sm–Nd and U–Pb systematics of single titanite grains. *Chem. Geol.* 261, 53–61.
- Baird, G.B., MacDonald, W., 2004. Deformation of the Diana syenite and Carthage-Colton mylonite zone: Implications for timing of Adirondack Lowlands deformation. *Geol. Soc. Am. Mem.* 197, 285–297.
- Bohlen, S., Valley, J.W., Essene, E., 1985. Metamorphism in the Adirondacks. I. Petrology, pressure and temperature. *J. Petrol.* 26, 971–992.
- Bonamici, C., Kozdon, R., Ushikubo, T., Valley, J.W., 2011. High-resolution P–T–t paths from  $\delta^{18}\text{O}$  zoning in titanite: A snapshot of late-orogenic collapse in the Grenville of New York. *Geology* 39, 959–962.
- Bonamici, C.E., Kozdon, R., Ushikubo, T., Valley, J.W., 2014. Intragrain oxygen isotope zoning in titanite by SIMS: Cooling rates and fluid infiltration along the Carthage-Colton Mylonite Zone, Adirondack Mountains, NY, USA. *J. Metamorph. Geol.* 32, 71–92.
- Carslaw, H.S., Jaeger, J.C., 1959. *Conduction of heat in solids*. 2nd ed. Clarendon Press, Oxford.
- Cartwright, I., Valley, J.W., Hazelwood, A.-M., 1993. Resetting of oxybarometers and oxygen isotope ratios in granulite facies orthogneisses during cooling and shearing, Adirondack Mountains, New York. *Contrib. Mineral. Petrol.* 113, 208–225.
- Chappell, J., Bickford, M.E., Selleck, B.W., Wooden, J., Mazdab, F.K., Heumann, M.J., 2006. High-temperature shearing and pegmatite formation during ottawan extensional collapse, northwestern Adirondack mountains, New York. *Geol. Soc. Am. Abstr. Programs* 38, 385.
- Cherniak, D.J., 1993. Lead diffusion in titanite and preliminary results on the effects of radiation damage on Pb transport. *Chem. Geol.* 110, 177–194.
- Cherniak, D.J., 1995. Sr and Nd diffusion in titanite. *Chem. Geol.* 125, 219–232.
- Cherniak, D.J., 2006. Zr diffusion in titanite. *Contrib. Mineral. Petrol.* 152, 639–647.
- Crank, J., 1975. *The mathematics of diffusion*. 2nd ed. Clarendon Press, Oxford.
- Dahl, P.S., Pomfrey, M.E., Foland, K.A., 2004. Slow cooling and apparent tilting of the Adirondack Lowlands, Grenville Province, New York (U.S.A.), based upon  $^{40}\text{Ar}/^{39}\text{Ar}$  ages. *Geological Society of America Memoir* 197, 299–324.
- Dodson, M., 1973. Closure temperature in cooling geochronological and petrological systems. *Contrib. Mineral. Petrol.* 40, 259–274.
- Donovan, J., Kremser, D., Fournelle, J.H., 2012. Probe for EPMA: acquisition, automation and analysis. Probe Software, Inc., Eugene, Oregon.
- Flowers, R., Mahan, K., Bowring, S.A., Williams, M., Pringle, M., Hodges, K., 2006. Multistage exhumation and juxtaposition of lower continental crust in the western Canadian Shield: linking high-resolution U–Pb and  $^{40}\text{Ar}/^{39}\text{Ar}$  thermochronometry with pressure–temperature–deformation paths. *Tectonics* 25, TC4003.
- Frost, B., Chamberlain, K., Schumacher, J., 2000. Sphene (titanite): phase relations and role as a geochronometer. *Chem. Geol.* 172, 131–148.
- Gao, X.-Y., Zheng, Y.-F., Chen, Y.-X., 2011. U–Pb ages and trace elements in metamorphic zircon and titanite from UHP eclogite in the Dabie orogen: constraints on P–T–t path. *J. Metamorph. Geol.* 29, 721–740.
- Geraghty, E.P., Isachsen, Y.W., Wright, S.F., 1981. Extent and character of the Carthage-Colton mylonite zone, northwest Adirondacks, New York. U.S. Nuclear Regulatory Commission Technical Report NUREG/CR-1865.
- Hamilton, M., McLelland, J., Selleck, B.W., 2004. SHRIMP U–Pb zircon geochronology of the anorthosite–mangerite–charnockite–granite suite, Adirondack Mountains, New York: Ages of emplacement and metamorphism. *Geol. Soc. Am. Mem.* 197, 337–356.
- Heumann, M.J., 2004. Thermochronological and Geochronological studies in the Adirondack Highlands and Lowlands. Syracuse University, Syracuse, New York.
- Higgins, J., Ribbe, P., 1976. The crystal chemistry and space groups of natural and synthetic titanites. *Am. Mineral.* 61, 878–888.
- Johnson, E., Selleck, B.W., 2005. The nature and significance of the Carthage-Colton Shear Zone and related late-to-post tectonic granites and ore deposits; Adirondack Mountains, New York. Friends of the Grenville Field Trip Guidebook.
- Johnson, E., Goergen, E., Fruechey, B.L., 2004. Right lateral oblique slip movements followed by post-Ottawan (1050–1020 Ma) orogenic collapse along the Carthage-Colton shear zone: Data from the Dana Hill metagabbro body, Adirondack Mountains, New York. In: Tollo, R.P., Corriveau, L., McLelland, J., Bartholomew, M.J. (Eds.), *Proterozoic tectonic evolution of the Grenville orogen in North America*, pp. 357–378.
- Kelly, J.L., Fu, B., Kita, N.T., Valley, J.W., 2007. Optically continuous silcrete quartz cements of the St. Peter Sandstone: High precision oxygen isotope analysis by ion microprobe. *Geochim. Cosmochim. Acta* 71, 3812–3832.
- Kita, N.T., Ushikubo, T., Fu, B., Valley, J.W., 2009. High precision SIMS oxygen isotope analysis and the effect of sample topography. *Chem. Geol.* 264, 43–57.
- Kitchen, N., Valley, J.W., 1995. Carbon isotope thermometry in marbles of the Adirondack Mountains, New York. *J. Metamorph. Geol.* 13, 577–594.
- Kohn, M.J., Corrie, S.L., 2011. Preserved Zr-temperatures and U–Pb ages in high-grade metamorphic titanite: Evidence for a static hot channel in the Himalayan orogen. *Earth Planet. Sci. Lett.* 311, 136–143.
- Kruckenber, S., Whitney, D., Fanning, C.M., Teyssier, C., Dunlap, W., 2008. Paleocene–Eocene migmatite crystallization, extension, and exhumation in the hinterland of the northern Cordillera: Okanogan dome, Washington, USA. *Geol. Soc. Am. Bull.* 120, 912–929.
- Lamb, W.M., 1993. Retrograde deformation within the Carthage-Colton Zone as recorded by fluid inclusions and feldspar compositions: tectonic implications for the southern Grenville Province. *Contrib. Mineral. Petrol.* 114, 379–394.
- Ludwig, K., 2012. *SQUID 2: A User's Manual*. 5. Berkeley Geochronology Center Special Publication, p. 110.
- Mazdab, F.K., 2009. Characterization of flux-grown trace-element-doped titanite using high-mass-resolution ion microprobe (SHRIMP-RG). *Can. Mineral.* 47, 813–831.
- McLelland, J., Selleck, B.W., Hamilton, M., Bickford, M.E., 2010. Late- to post-tectonic setting of some major Proterozoic anorthosite–mangerite–charnockite–granite (AMCG) suites. *Can. Mineral.* 48, 729–750.
- Mezger, K., Rawnsley, C., Bohlen, S., Hanson, G., 1991a. U–Pb garnet, sphene, monazite, and rutile ages: Implications for the duration of high-grade metamorphism and cooling histories, Adirondack Mts., New York. *J. Geol.* 99, 415–428.
- Mezger, K., van der Pluijm, B., Essene, E., Halliday, A., 1991b. Synorogenic collapse: a perspective from the middle crust, the Proterozoic Grenville Orogen. *Science* 254, 695–698.
- Mezger, K., van der Pluijm, B., Essene, E., Halliday, A., 1992. The Carthage-Colton Mylonite Zone (Adirondack Mountains, New York): The Site of a Cryptic Suture in the Grenville Orogen? *J. Geol.* 100, 630–638.
- Morishita, Y., Giletti, B., Farver, J., 1996. Volume self-diffusion of oxygen in titanite. *Geochem. J.* 30, 71–80.
- Oberti, R., Smith, D., Rossi, G., Caucia, F., 1991. The crystal-chemistry of high-aluminium titanites. *Eur. J. Mineral.* 3, 777–792.
- Scott, D., St-Onge, M., 1995. Constraints on Pb closure temperature in titanite based on rocks from the Ungava orogen, Canada: Implications for U–Pb geochronology and P–T path determinations. *Geology* 23, 1123–1126.
- Selleck, B.W., McLelland, J., Bickford, M.E., 2005. Granite emplacement during tectonic exhumation: The Adirondack example. *Geology* 33, 781–784.
- Shang, C., Morteani, G., Satir, M., Taubald, H., 2010. Neoproterozoic continental growth prior to Gondwana assembly: Constraints from zircon–titanite geochronology, geochemistry and petrography of ring complex granitoids, Sudan. *Lithos* 118, 61–81.
- Spencer, K.J., Hacker, B.R., Kylander-Clark, A.R.C., Andersen, T.B., Cottle, J.M., Stearns, M.A., Poletti, J.E., Seward, G.G.E., 2013. Campaign-style titanite U–Pb dating by laser-ablation ICP: Implications for crustal flow, phase transformations and titanite closure. *Chem. Geol.* 341, 84–101.
- Storey, C., Smith, M., Jeffries, T., 2007. In situ LA-ICP-MS U–Pb dating of metavolcanics of Norrbotten, Sweden: Records of extended geological histories in complex titanite grains. *Chem. Geol.* 240, 163–181.
- Storm, L., Spear, F., 2005. Pressure, temperature and cooling rates of granulite facies migmatitic pelites from the southern Adirondack Highlands, New York. *J. Metamorph. Geol.* 23, 107–130.
- Streepey, M., van der Pluijm, B., Essene, E., Hall, C., Magloughlin, J., 2000. Late Proterozoic (ca. 930 Ma) extension in eastern Laurentia. *Geol. Soc. Am. Bull.* 112, 1522–1530.
- Streepey, M., Johnson, E., Mezger, K., van der Pluijm, B., 2001. Early History of the Carthage-Colton Shear Zone, Grenville Province, Northwest Adirondacks, New York (USA). *J. Geol.* 109, 479–492.
- Tiepolo, M., Oberti, R., Vannucci, R., 2002. Trace-element incorporation in titanite: constraints from experimentally determined solid/liquid partition coefficients. *Chem. Geol.* 191, 105–119.
- Tilton, G., Grunefelder, M., 1968. Sphene: Uranium–lead ages. *Science* 159, 1458.
- Valley, J.W., Kita, N.T., 2009. In situ oxygen isotope geochemistry by ion microprobe. In: Fayek, M. (Ed.), *Secondary ion mass spectrometry in the earth sciences*. Mineralogical Society of Canada Short Course, pp. 19–63.
- Valley, P.M., Hanchar, J.M., Whitehouse, M.J., 2011. New insights on the evolution of the Lyon Mountain Granite and associated Kiruna-type magnetite–apatite deposits, Adirondack Mountains, New York State. *Geosphere* 7, 357–389.
- Verts, L., Chamberlain, K., Frost, C., 1996. U–Pb sphene dating of metamorphism: the importance of sphene growth in the contact aureole of the Red Mountain pluton, Laramie Mountains, Wyoming. *Contrib. Mineral. Petrol.* 125, 186–199.
- Warren, C.J., Grujic, D., Cottle, J.M., Rogers, N.W., 2012. Constraining cooling histories: rutile and titanite chronology and diffusion modelling in NW Bhutan. *J. Metamorph. Geol.* 30, 113–130.
- Wiener, R., 1983. Adirondack Highlands–Northwest Lowlands “boundary”: A multiply folded intrusive contact with fold-associated mylonitization. *Geol. Soc. Am. Bull.* 94, 1081–1108.
- Zhang, X., Cherniak, D.J., Watson, E.B., 2006. Oxygen diffusion in titanite: lattice diffusion and fast-path diffusion in single crystals. *Chem. Geol.* 235, 105–123.